Multidecadal-Scale Freshening at the Salinity Minimum in the Western Part of North Pacific: Importance of Wind-Driven Cross-Gyre Transport of Subarctic Water to the Subtropical Gyre

TAKUYA NAKANOWATARI AND HUMIO MITSUDERA

Institute of Low Temperature Science, Hokkaido University, Sapporo, Hokkaido, Japan

TATSUO MOTOI

Meteorological College, Kashiwa, Chiba, Japan

ICHIRO ISHIKAWA

Japan Meteorological Agency, Tokyo, Tokyo, Japan

KAY I. OHSHIMA AND MASAAKI WAKATSUCHI

Institute of Low Temperature Science, Hokkaido University, Sapporo, Hokkaido, Japan

(Manuscript received 12 December 2013, in final form 24 December 2014)

ABSTRACT

Using oceanographic observations and an eddy-resolving ice–ocean coupled model simulation from 1955 to 2004, the effects of the wind-driven ocean circulation change that occurred in the late 1970s during multidecadal-scale freshening of the North Pacific Intermediate Water (NPIW) at salinity minimum density (~26.8 σ_θ) were investigated. An analysis of the observations revealed that salinity decreased significantly at the density range of 26.6–26.8 σ_θ in the western subtropical gyre, including the mixed water region (MWR). The temporal variability of the salinity is dominated by the marked change in the late 1970s. With results similar to the observations, the model, selectively forced by the interannual variability of the wind-driven ocean circulation, simulated significant freshening of the intermediate layer over the subtropical gyre. The significant freshening is related to the increase in southward transport of the Oyashio associated with the intensification of the Aleutian low. Accompanying these changes, the intrusion of fresh and low potential vorticity water, originating in the Okhotsk Sea, to the MWR increased, and the freshening signal propagated farther southward in the western subtropical gyre during the subsequent 6 yr, crossing the Kuroshio Extension. These results indicate that the multidecadal-scale freshening of the NPIW is partly caused by intensification of the wind-driven cross-gyre transport of the subarctic water to the subtropical gyre.

1. Introduction

North Pacific Intermediate Water (NPIW) occupies the subtropical gyre region of the North Pacific and has well-defined low salinity at a depth range of 300–800 m (Sverdrup et al. 1942) and a distinct salinity minimum centered in the narrow density range of σ_θ = 26.7–26.9 (Reid 1965). Ventilation areas for the NPIW have been identified in subpolar regions, mainly in the Sea of Okhotsk (Yasuda 1997) and the Gulf of Alaska (Van Scoy et al. 1991; You et al. 2000). Ventilated water in the Sea of Okhotsk is characterized by a pycnostad and is known as Okhotsk Sea Mode Water (Yasuda 1997) or Okhotsk Sea Intermediate Water (OSIW) (Itoh et al. 2003). Ventilated waters in these regions are transformed along the subarctic–subtropical frontal zone, which sets the NPIW density partly by cabelling (which describes sinking water resulting from lateral mixing) (Talley and Yun 2001; You 2003; Yun and Talley 2003).

Corresponding author address: Takuya Nakanowatari, Japan Agency for Marine-Earth Science and Technology, 2-15 Natsushima-cho, Yokosuka, 237-0061, Japan.
E-mail: nakanow@jamstec.go.jp

DOI: 10.1175/JPO-D-13-0274.1

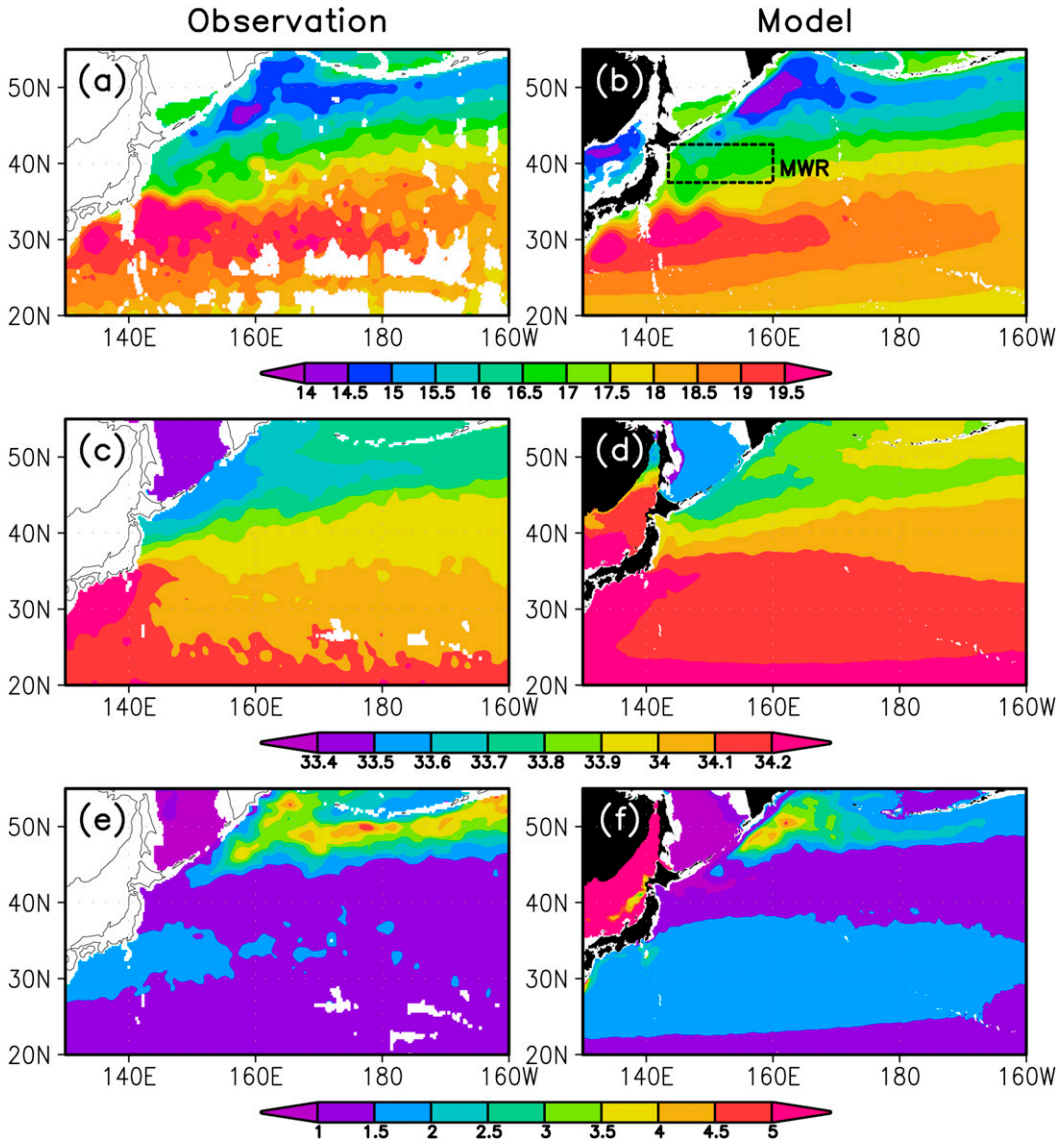

FIG. 1. Climatologies of (a),(b) acceleration potential, (c),(d) salinity, and (e),(f) PV at 26.8 σ_θ for (left) the observations and (right) the model simulation. The contour interval is (top) 0.5 $m^2 s^{-2}$, (middle) 0.1 psu, and (bottom) $0.5 \times 10^{-10} m^{-1} s^{-1}$. The acceleration potential is calculated relative to 2000 dbar. In (b), the region for the MWR (broken line) is indicated.

Unlike other major intermediate water masses, such as Antarctic Intermediate Water and Labrador Sea Water, the NPIW lacks a corresponding oxygen maximum core and density $> 26.8\ \sigma_\theta$ does not outcrop in the formation area (Talley and Nagata 1995). Thus, the isopycnal mixing processes between the subarctic and subtropical waters, and the direct ventilation areas, are essential for NPIW formation.

From climatological data analysis, Talley (1993) showed that cold and fresh waters are confined to the region between the Kuroshio Extension (KE) and the Oyashio Front [referred to as the mixed water region (MWR); see Fig. 1b] and suggested that NPIW is formed mainly in this region. Mitsudera et al. (2004) used a high-resolution regional ocean model to make a detailed diagnosis of how the mesoscale current system in the MWR leads to southward transport of OSIW. Their study showed that southward intrusion of the Oyashio plays a leading role in the southward transport of OSIW in the MWR. Kouketsu et al. (2005) showed that mesoscale eddies generated by baroclinic instability waves created between the subtropical and subarctic water boundaries also reinforce isopycnal mixing between these. Eddy-resolving ocean general circulation model

(OGCM) simulation supports the significant roles of the mesoscale eddies and southward Oyashio intrusion in transporting the OSIW southward (Ishikawa and Ishizaki 2009; Fujii et al. 2013).

The variability of the NPIW is important for freshwater transport (Talley 2008) and the circulation of materials and heat (Talley 2003) in the North Pacific. For example, silicate, which is abundant in the subarctic North Pacific, is transported effectively to low latitudes through the NPIW pathway (Sarmiento et al. 2004). It has also been reported that iron, an essential micronutrient for phytoplankton, originates from the OSIW and may lead to abundant biological productivity in the North Pacific (Nishioka et al. 2007). Furthermore, long-term changes in the water mass are likely to be crucial for the carbon cycle and pertinent to global warming issues. The net anthropogenic CO_2 flux from the Okhotsk Sea to the Pacific is estimated to be $0.025\,\mathrm{GtC\,yr^{-1}}$, and a large part of this flux ($0.02\,\mathrm{GtC\,yr^{-1}}$) enters the intermediate depth of the subtropical gyre and thus the NPIW (Yasuda et al. 2002). This flux explains approximately 15% of the inventory in the North Pacific.

It has recently been reported that there was a significant freshening of NPIW salinity in the latter half of twentieth century (the water mass was cooled on its isopycnal surfaces) (Wong et al. 1999, 2001; Joyce and Dunworth-Baker 2003; Kouketsu et al. 2007; Nakano et al. 2007). By comparing hydrographic observations from the 1960s and 1985–94, Wong et al. (1999, 2001) suggested that fresher surface water feeds into ventilation regions such as the Okhotsk Sea and Alaska Gyre and that their signals are advected along the formation pathway of NPIW. In addition, several studies have indicated that freshening in the surface water of the subarctic North Pacific (Durack and Wijffels 2010) and the Sea of Okhotsk (Hill et al. 2003; Ohshima et al. 2014) occurs on a multidecadal time scale, implying that freshened source water could modify the NPIW.

However, the above scenario, attributing freshening of the NPIW at the salinity minimum density with a center of 26.8 σ_θ (hereinafter, we refer to this as NPIW) to freshening at its sources, is questionable. Unlike the circumstance in the Southern Ocean, the MWR, which is the formation region for NPIW, does not outcrop even in winter (Talley 1993); thus, different physical mechanisms are involved in the formation of NPIW with density heavier than 26.8 σ_θ. The source water of NPIW heavier than 26.8 σ_θ is mainly subject to the ventilation processes in the Sea of Okhotsk (You et al. 2000). In the northwestern shelf region, sea ice production leads to the production of cold, oxygen-rich dense shelf water (DSW) with densities up to 27.0 σ_θ (Shcherbina et al. 2003). The DSW is transported southward into the intermediate layer in the southern Okhotsk Sea by the East Sakhalin Current (Mizuta et al. 2003) and isopycnally mixed with intermediate water coming from the North Pacific (Yasuda 1997; Itoh et al. 2003). This mixing forms OSIW, which is the coldest, freshest, and most oxygen-rich water in the North Pacific, on 26.8–27.4 σ_θ isopycnals (Talley 1991). The freshening of surface water would tend to shift the core density of DSW (26.8 σ_θ) to a lighter density. Thus, there is a possibility that the freshening of surface water leads to a reduction in DSW on the salinity minimum density surface of NPIW and results in a warming and salinification of OSIW (Matsuda et al. 2009; Nakanowatari et al. 2014).

Between 1955 and 2004, the potential temperature in the Sea of Okhotsk and the western subarctic region increased significantly on 26.8–27.2 σ_θ isopycnals, which translated to a salinification signal on isopycnal surfaces due to the surrounding temperature–salinity (T–S) curve (Itoh 2007; Nakanowatari et al. 2007). These studies suggest that ventilation of the intermediate layer in the subarctic region including the Sea of Okhotsk has been weakened. This hypothesis is also supported by a decrease in levels of dissolved oxygen in the Sea of Okhotsk (Nakanowatari et al. 2007), Oyashio region (Ono et al. 2001), and the western subarctic gyre (Andreev and Watanabe 2002; Emerson et al. 2004). Because the weakening ventilation leads to a shift in the densities that are ventilated, this change may be related to the freshening signal in NPIW at the density range lighter than 26.8 σ_θ. However, at the salinity minimum density range for NPIW, the freshening signals in NPIW on isopycnal surfaces are not accomplished by the isopycnal mixing processes of the salinification signal of OSIW on the corresponding isopycnal surface.

An alternative interpretation of the freshening in NPIW suggests a possible role of the wind-driven ocean circulation change. Previous observational and modeling studies have suggested that interannual variability of southward Oyashio transport is related to wintertime changes in basin-scale wind stress (Sekine 1988; Isoguchi et al. 1997; Nonaka et al. 2008). The atmospheric variability over the North Pacific bears a half-century scale change characterized by the deepened Aleutian low of 1976/77 (Nitta and Yamada 1989; Trenberth 1990), which is known to be a part of the periodic change of the Pacific decadal oscillation (PDO) characterized by a basinwide scale change in sea surface temperature (SST) and sea level pressure (SLP) (Mantua et al. 1997; Minobe 1997). Therefore, such a shift in the wind stress may have enhanced southward transport of the Oyashio water in the MWR and led to the freshening in the NPIW in the latter half of twentieth century.

The importance of the wind-driven ocean circulation change for the water mass properties of the intermediate

water has been indicated by several numerical studies. Auad et al. (2003) showed in an ocean model simulation that when the wind stress curl strengthened after the climate regime shift that occurred in 1976/77, a reduction in salinity occurred along the northern boundary of the NPIW. They suggested that the change resulted from anomalous southeastward flow of cold and low-salinity waters from the Sea of Okhotsk. On the other hand, Nakano et al. (2005) indicated that the region of westward flow south of the Kuroshio Extension became fresher as a result of the strengthened subtropical gyre. However, these studies were based on models that had spatial resolutions that were inadequate for representing the Oyashio and mesoscale eddies (which are crucial for the formation of NPIW) (Ishikawa and Ishizaki 2009; Tanaka et al. 2010). In this study, we examine the role of the wind-driven ocean circulation change on multidecadal-scale change in the NPIW at the salinity minimum density of 26.8 σ_θ in the western subtropical gyre and its possible mechanisms, using historical oceanographic data and an eddy resolving, ice–ocean, coupled model simulation selectively forced by the interannual variability of the wind-driven ocean circulation. We show with the simulation that the observed multidecadal-scale change in the NPIW property (freshening on the isopycnal surface) originates from the MWR extending to the subtropical recirculation across the Kuroshio Extension. The observed and simulated data in the Sea of Okhotsk, which is a major source region for NPIW, do not support that freshening in the source water is essential for the multidecadal-scale freshening of NPIW. In light of the observed and simulated changes in the source region, these model results are a satisfactory implication that the NPIW freshening is caused mainly by intensification of the wind-driven cross-gyre transport of the subarctic water to the subtropical gyre.

The paper is organized as follows: Section 2 describes the model and observational data, section 3 evaluates the climatological representation of the model in comparison with the observational data, and section 4 shows the observed multidecadal-scale change in the water properties of the NPIW and compares this with the simulated data. In section 5, possible mechanisms for the change in the NPIW are examined based on the simulated data, with an emphasis on changes in the wind-driven gyre circulation. Section 6 provides a summary and discussion.

2. Model output and observational data

The model simulation data used in this study were integrated using an eddy-resolving ($^1/_{12}^\circ$ grid) ice–ocean coupled model of the North Pacific developed at the Meteorological Research Institute, Japan Meteorological Agency. The model simulation is outlined briefly here, and a detailed description is available in Ishikawa and Ishizaki (2009). The model solves a primitive equation system with a vertical σ–z hybrid coordinate, free-surface, and Boussinesq and hydrostatic approximations. To realistically simulate the variation processes in the Sea of Okhotsk, a sea ice model based on Mellor and Kantha (1989) with elastic–viscous–plastic (EVP) dynamics (Hunke and Ducowicz 1997) is applied. In addition, the tidal mixing process, which is also important for the formation of the Okhotsk Sea Intermediate Water and the NPIW (Nakamura et al. 2006), is represented in the form of parameterization of the vertical diffusivity coefficient (St. Laurent et al. 2002). It is noted that this parameterization has no bidecadal modulation of the tidal cycle reported by Yasuda et al. (2006). There are 62 levels in the vertical direction with increasing thickness in the deep layers (27 layers from the surface to a depth of 500 m). The model domain occupies the entire North Pacific (from 15°S to 65°N and from 100°E to 75°W).

TABLE 1. Difference of salinity on isopycnal surfaces between 1977–2004 and 1955–76 averaged over the western subtropical gyre. Bold numbers indicate the differences that exceed the 95% confidence levels based on the Student's t test.

σ_θ	26.6	26.7	26.8	26.9	27.0	27.1
Obs	**−0.030**	**−0.022**	**−0.012**	−0.001	0.005	**0.008**
Model	**−0.035**	**−0.031**	**−0.025**	**−0.017**	**−0.008**	0.000

The model was first integrated for a period of 70 yr using *World Ocean Atlas 1998* (*WOA98*) climatological temperature (Antonov et al. 1998) and salinity (Boyer et al. 1998) under the climatological monthly-mean atmospheric forcing of NCEP–NCAR Reanalysis-2 data from the period 1979–2003 (Kanamitsu et al. 2002). Surface heat fluxes are calculated by the bulk formulae, and freshwater fluxes are estimated from evaporation minus precipitation and river runoff. Sea surface salinity (SSS) is restored with an 8-day damping time scale to avoid the problem of SSS drifting using climatological monthly-mean data. Temperature and salinity are restored for the southern boundary using climatological monthly-mean data. To evaluate SSS drifting, the simulated change in SSS averaged over the entire model region is calculated using the difference between the former (1955–76) and latter periods (1977–2004). The change in SSS from the former to latter period is 0.0011 psu, one order less than the salinity difference values, which ranged from −0.01 to −0.03 psu, discussed in this study (Table 1).

Following this spinup, model integration was conducted with 6-hourly atmospheric fields of the NCEP–NCAR reanalysis data from 1949 to 2005 (Kalnay et al.

1996). In this integration, SSS was restored to the climatological monthly mean to remove the interannual variation in thermohaline processes in the North Pacific. Thus, this experiment is considered to be selectively forced by the interannual variability of the wind-driven ocean circulation. The absence of the interannual variability in thermohaline change is discussed in section 4. For the following analysis, we used the model's monthly climatology defined as the mean from 1955 to 2004 and anomalies defined as deviations from the mean during the same time period because unrealistic gaps occur for the first several years. For analytical convenience, the full-resolution model output for the model data was reduced to 1° resolution, but it should be noted that this has no effect on the results of the gyre-scale phenomena on interdecadal time scales.

To evaluate the model simulation and the multidecadal variation of the NPIW, we used gridded data of potential temperature, salinity, potential vorticity (PV), and acceleration potential on isopycnal surfaces. This dataset was based on oceanographic observations from the *World Ocean Database 2001* (*WOD2001*) (Conkright et al. 2002), profiling float data obtained by the international Argo program from 2000 to 2004, the Japan–Russia–United States international joint study of the Sea of Okhotsk from 1998 to 2004, and the Japan Oceanographic Data Center. For *WOD2001*, we adopted profiles at observation levels at which both temperature and salinity were available. The spatial coverage was the entire North Pacific (15°–65°N, 135°–120°W), a larger coverage than that produced by Nakanowatari et al. (2007).

The quality control and gridded method adopted in this study were similar to those of earlier studies (Itoh et al. 2003). Hydrographic data at discrete depths, mostly from bottle samples, were linearly interpolated to a 1-m interval, and then the values of the potential temperature, salinity, isopycnal layer thickness, and isopycnal depth were selected at 0.1 σ_θ intervals from 26.6 to 27.1 σ_θ. The isopycnal layer thickness h is defined by the distance for ± 0.05 σ_θ of each isopycnal surface. [i.e., $h(\sigma_\theta) = \int_{z(\sigma_\theta - 0.05)}^{z(\sigma_\theta + 0.05)} dz$].

Before we applied the quality control, we divided all of the data into two parts, one set for the Okhotsk and another for the Pacific Ocean because the water mass properties differ considerably between the two oceans. To perform the quality control check, the data were first divided into 60-km geographical squares. Within each geographical bin, the mean and the standard deviation of the potential temperature, salinity, isopycnal layer thickness, and depth were calculated. Then, data that fell outside the 2.5 interval were eliminated. The quality check procedure above was further performed for larger geographical bins, specifically by using 200- and 400-km geographical squares. The resulting data in the analyzed region were 182 230 stations at 26.8 σ_θ.

Annual-mean climatology was calculated using a 0.25° × 0.25° latitude/longitude grid, with a method similar to that of Levitus and Boyer (1994). To calculate a grid value of the annual-mean climatology from the station data, we used the Gaussian distribution as a weight function with an *e*-folding scale of 75 km and an influence radius of 150 km to resolve regional features in the Sea of Okhotsk and the boundary current and fronts in the Kuroshio–Oyashio Confluence (KOC). An *e*-folding scale of 75 km can be fit to the autocorrelation functions on each isopycnal bin in and around the Sea of Okhotsk (Itoh et al. 2003). If the number of observations within the influence radius was less than 5, that grid box was regarded as having no data. Annual-mean anomalies were gridded using simple averaging of anomalies as the differences of the observed values from the climatologies over a yearly 2.5° × 2.5° grid box from 1955 to 2004. Neither spatial interpolation nor spatial smoothing was applied to the anomaly field.

To examine the temporal variability of potential temperature in the NPIW before 1955, we produced annual-mean anomalies of the potential temperature at isopycnal surfaces extending back to 1925 based on oceanographic observations from the *World Ocean Database 2001* (Conkright et al. 2002). These data are referred to as the historical data. For the index of wind stress over the North Pacific, we used the North Pacific index [NPI; the area-averaged sea level pressure over the region 30°–65°N, 160E°–140°W (the rectangular region shown in Fig. 13d)] in December to the following May (Trenberth and Hurrell 1994). Negative values of the NPI correspond to a deeper-than-normal Aleutian low pressure system, accompanied by enhanced westerly winds across the central North Pacific and strengthened southerly (northerly) flow over the eastern (western) North Pacific; opposite conditions are obtained for positive values.

3. Climatological features of the model simulation

In this section, we assess both the representation of the intermediate water circulation and the water properties in the model simulation by comparing climatological data with those of observations. The model representation of NPIW is also shown in Ishikawa and Ishizaki (2009), but we here focus on the representation of the frontal and jet structures in the MWR. For the climatological features given by the model, we show the annual-mean data from spinup, which are not spatially interpolated.

To evaluate the intermediate water circulation, we adopted the acceleration potential, which is the dynamical height at an isopycnal surface. Figure 1 (top panels)

shows the acceleration potential at 26.8 σ_θ, which corresponds to the core density of the NPIW. We can see that the model successfully simulates many realistic features of the Kuroshio Extension and Oyashio Front in the intermediate layer. The Kuroshio, which is the western boundary current of the subtropical gyre, is successfully separated south of Japan and forms the Kuroshio Extension along 32°N in the model. Accompanied by the separation of the Kuroshio, a southward intrusion of the Oyashio (characterized by the contour of $17\,m^2\,s^{-2}$) reaches 35°N along the western boundary, indicating that the southward intrusion of the Oyashio is well represented in this model. These current systems generally are not fully represented in coarse-resolution ocean models.

The climatological salinity and PV (middle and bottom panels in Fig. 1) show that the water mass properties of the NPIW and the source water (OSIW) at 26.8 σ_θ are also well simulated by the model (see also Ishikawa and Ishizaki 2009). The relatively low salinity (less than 33.5) and low PV (less than $1.0 \times 10^{-10}\,m^{-1}\,s^{-1}$) water in the southern part of the Sea of Okhotsk can be distinguished from the high-salinity and high-PV subarctic water (Figs. 1c,e). These water properties are also found in the simulated data (Figs. 1d,f), although the simulated salinity is somewhat higher than the observed salinity. Simulated water salinity less than 33.5, which corresponds to the modified DSW, occurs east of Sakhalin Island, indicating that the property of OSIW in the model is climatologically sustained by brine rejection in winter. The low-salinity tongue of NPIW (shown by the salinity contour of 34.1 in Fig. 1c) is extended westward along the recirculation of the subtropical gyre south of the Kuroshio Extension (shown by the contour of $19\,m^2\,s^{-2}$ in Fig. 1a). These distributions of salinity and acceleration potential are also apparent in the simulation (Figs. 1d,b). It is also noted that the patch-like structure of salinity around the Kuroshio Extension does not occur in the model simulation, which could be attributable to mesoscale eddies that were not filtered out in the climatological observations because the influence radius of the weight function used in this study is smaller than that of Levitus and Boyer (1994).

4. Multidecadal-scale change in NPIW: Observed versus model

We begin by examining the spatial pattern of multidecadal-scale freshening at the salinity minimum density of the NPIW, which has not been fully examined in previous studies. In general, the freshening signal can have a different response on density surfaces, depending on the vertical structure of the T–S properties (Bindoff and McDougall 1994, 2000). In the case of the subtropical gyre region, the freshening signal at the salinity minimum density of NPIW can be translated to both a cooling and freshening signal on isopycnal surfaces due to the surrounding T–S curve (e.g., Nakano et al. 2005). Hereafter, therefore, we examine changes in the NPIW using salinity on the isopycnal surface. This analysis can remove the apparent changes in salinity caused by isopycnal movement. To evaluate the effect of the regime shift in the wind stress, the multidecadal-scale change of salinity was calculated using the difference between 1955–76 and 1977–2004. The difference between these periods shows a rate of change over approximately 35 yr, which ensures that the effect of bidecadal variability (Kouketsu et al. 2010) is removed from the analysis. It is noted that the choice of the analyzed period for the difference (e.g., the difference between 1955–79 and 1980–2004) does not essentially affect our results.

The observed difference of salinity at the salinity minimum density of NPIW (26.8 σ_θ) shows broad-scale freshening over the subtropical gyre (Fig. 2a). Pronounced negative anomalies are confined to the western subtropical gyre, and less prominent negative anomalies exist in the eastern part of the North Pacific, although hydrographic observations are not fully available in this region. In the northern North Pacific, positive anomalies occur in the western subarctic gyre (including the Sea of Okhotsk and the Alaska gyre). The positive anomalies in the Sea of Okhotsk are consistent with the warming trend on the corresponding isopycnal surfaces from 1955 to 2004 (Nakanowatari et al. 2007).

The difference appears to provide a reasonable representation of the multidecadal-scale change, although observational data are not fully available throughout the analyzed period. A local two-sided Student's t test was performed separately for the mean fields of both the former and latter period, assuming the annual mean of the potential temperature field as temporally independent. According to this test, the negative anomalies were statistically significant at the 95% confidence level over most of the western subtropical gyre (Fig. 2a).

Changes in the salinity of the NPIW on other isopycnal surfaces were also examined. For the representation of the NPIW, we used area averaging over the western subtropical gyre region (shown in Fig. 2a). The vertical profile of the change in salinity indicates that the freshening is statistically significant at 26.6–26.8 σ_θ (Table 1). Such a freshening signal over the subtropical gyre is weaker at surfaces with higher densities. These results are consistent with analyses of hydrographic data along meridional (about 25°N) and zonal (about 137°E) sections (Kouketsu et al. 2007; Nakano et al. 2007).

A map of the model's differences (Fig. 2b) also shows a significant freshening in the western subtropical gyre,

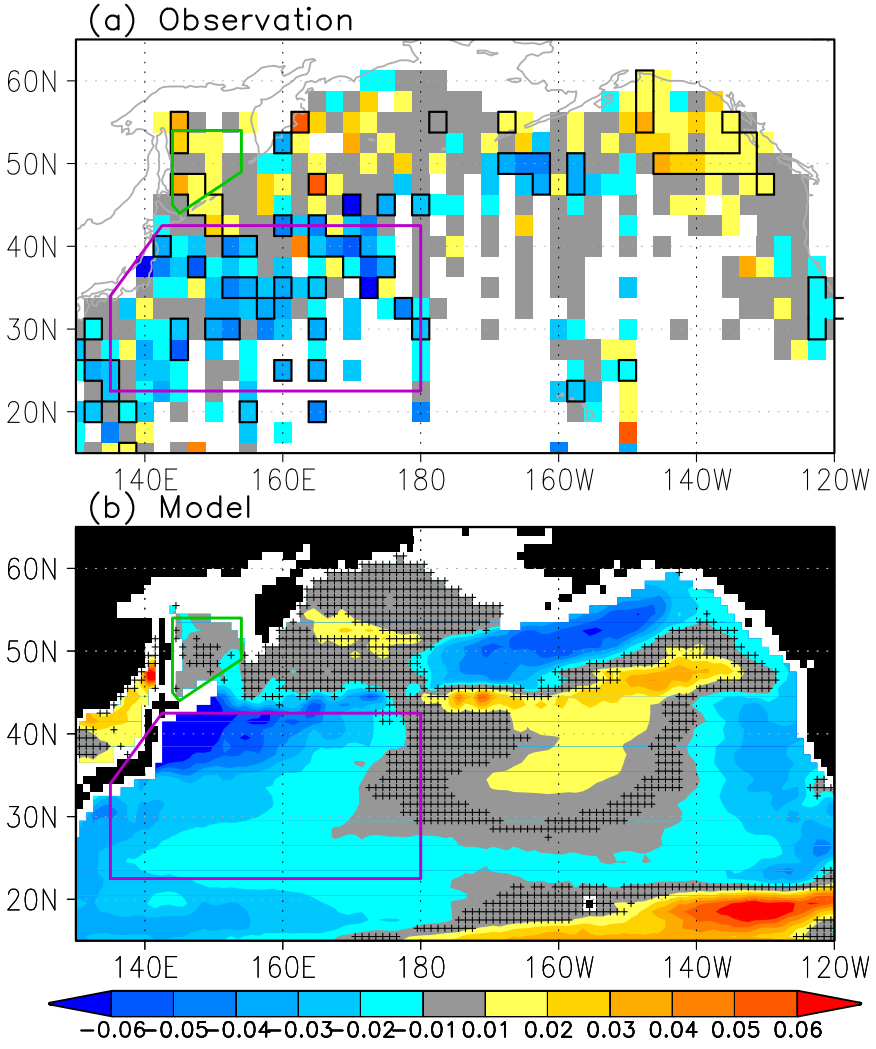

FIG. 2. Spatial pattern of change in the annually averaged salinity from 1955–76 to 1977–2004 at 26.8 σ_θ for (top) the observations and (bottom) the model simulation. The colors indicate the amplitude of the difference. Negative values indicate that potential temperature decreased from 1955–76 to 1977–2004. (a) The black grid box boundary indicates a region where the difference is significant at the 95% confidence level. In (a), the grid boxes where yearly temperature anomalies are not available for more than 5 yr in each period are not used for the analysis. (b) The region for insignificant difference is marked by the cross hatching. The statistical significance of the difference is based on a Student's t test distribution with 1 degree of freedom yr^{-1}. The boundaries of the western subtropical region (purple) and the Sea of Okhotsk (green), for which area-averaged quantities are displayed in Fig. 3, are indicated.

where the negative anomalies extend from the MWR around 40°N to the southern edge of the subtropical gyre (~20°N). The vertical profile for the change in the area-averaged salinity over the western subtropical gyre also shows the significant change at about the salinity minimum density (26.6–27.0 σ_θ) (Table 1), which is roughly consistent with the observed data.

However, there are some large-scale differences in the two maps (Figs. 2a,b). First, the center of the freshening is south of the Kuroshio Extension in the observations but north of it in the model; that is, in the model, the strongest freshening is in the MWR. This difference is probably related to underestimation of the simulated southward transport of the Oyashio water, as indicated by Ishikawa and Ishizaki (2009) who showed that the southward transport of the Oyashio water across 40°N west of 150°E is 2.6 Sverdrups (Sv; 1 Sv $\equiv 10^6\,\mathrm{m^3\,s^{-1}}$) between 26.6 and 27.4 σ_θ, which is about half the value based on the hydrographic data with the ADCP-referenced method reported by Shimizu et al. (2003)

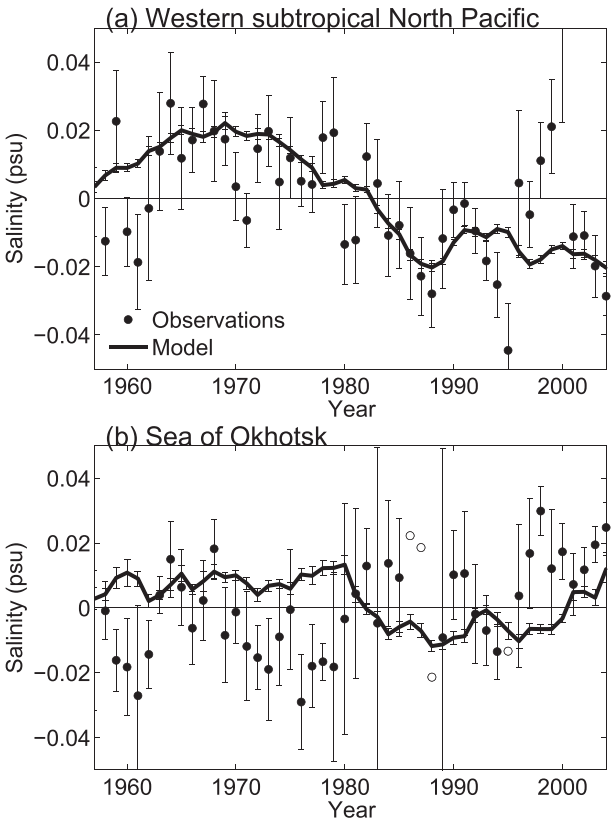

FIG. 3. Time series of annual-mean salinity anomalies at 26.8 σ_θ averaged over (a) the western subtropical North Pacific and (b) the Sea of Okhotsk (rectangular regions denoted by purple and green lines in Fig. 2a) for observations (circles) and model (solid line). A vertical line represents a ±1 standard error of the annual mean of the observation. In (b), open circles indicate the anomalies for the area, in which the number of the data is very small.

and about a quarter of that given by Masujima et al. (2003). Therefore, the Oyashio water in the MWR is not fully transported southward across the KE resulting in accumulation north of the KE.

Second, the salinity increased in the western subarctic gyre and Sea of Okhotsk in the observations, but this signal was not reproduced by the model. The chief discrepancy between Figs. 2a and 2b appears to be the absence of positive anomalies in the Sea of Okhotsk in the model. Even if we examine the salinity on the isopycnal surfaces of heavier densities, in which the warming in the Sea of Okhotsk is prominent (Itoh 2007), such a significant salinification signal is not found in the model simulation (not shown). Instead of it, the time series of the salinity anomalies in the model simulation show a transient gap in 1978/79 with small variance relative to the observed data (Fig. 3b). The transient gap might be related to inadequate representation of the interannual variability of dense shelf water formation over the northwestern shelf region because the NCEP–NCAR reanalysis data in the Sea of Okhotsk are not reliable during half of the simulated period (from 1949 to 1978) (Nakanowatari et al. 2010). On the other hand, the small variance of the simulated salinity anomalies is partly related to underestimation of the brine rejection of sea ice formation because the simulated SSS is restored to the climatological value. Thus, the absence of the salinification signal in the simulated data may be related to the fact that the effect of the interannual variation in thermodynamic processes in the Sea of Okhotsk is subtracted in this model simulation. Nevertheless, the overall consistency in the observed and simulated freshening in the NPIW suggests that the salinity change in OSIW has a negligible effect on this phenomenon.

Figure 3 compares the time series of annually averaged salinity at 26.8 σ_θ averaged over the western subtropical gyre for both the observations and the model simulation. The most apparent dominant feature is the low-frequency variation, which is characterized by positive anomalies from 1955 to 1976 and negative anomalies from 1977 to 2004. The correlation between these is 0.87 (significant at the 95% confidence level based on a Monte Carlo simulation using a phase randomization technique generating 1000 surrogate time series), indicating that the model realistically represents the multidecadal-scale change in the NPIW. However, the standard errors of the area-averaged time series in the observed data appear to be relatively large. As transient eddies are prominent in this area, this is probably related to the insufficient spatial coverage of the observed data. It is noted that an abrupt positive anomaly occurs in the observational data between 1998 and 2000. Because the sea surface temperature over the Kuroshio Extension area was significantly warmed in 1998/99 (Bond et al. 2003), this positive anomaly may be related to meandering of the Kuroshio Extension and/or warm and saline eddy shedding. The altimeter data also show that the sea surface height is relatively high along the northern boundary of the Kuroshio Extension in 1998/99 (not shown). In this model simulation, such a positive anomaly of potential temperature is obscure.

Bindoff and McDougall (1994, 2000) pointed out the possibility that warming of the water mass in the subtropical region can be translated to cooling and freshening on density surfaces, depending on the slope of the temperature and salinity profiles. To check whether the freshening at the salinity minimum density of NPIW is related to the warming signal, we examined the *T*–*S* properties of NPIW and OSIW for the past (1955–76) and present (1977–2004). The *T*–*S* properties of NPIW and OSIW in these two periods were calculated from the area-averaged values of potential temperature and salinity on isopycnal surfaces with grid box weights in the

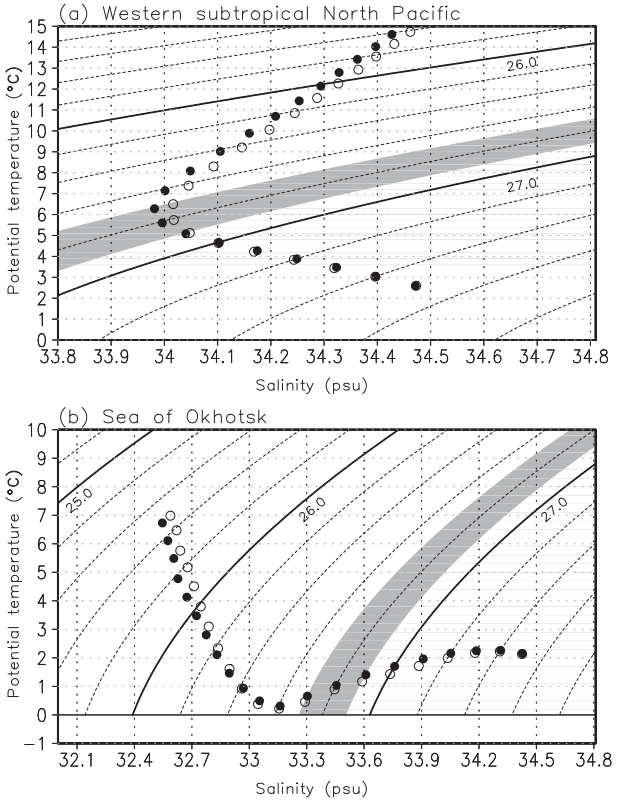

FIG. 4. Time variations of the observed *T*–*S* curve averaged over (a) the western subtropical North Pacific and (b) the Sea of Okhotsk (rectangular regions denoted by purple and green lines in Fig. 2a). Open (closed) circles denote the past (1955–76) and present (1977–2004) values on isopycnal surfaces. The shading indicates the density range of the salinity minimum core from 26.7 to 26.9 σ_θ.

western subtropical North Pacific and the Sea of Okhotsk (rectangular regions denoted by purple and green lines in Fig. 2a). The undefined value is not accounted for in this calculation. The observed salinity in the salinity minimum density range (26.7 to 26.9 σ_θ) is freshened, and the density for the salinity minimum decreases somewhat from 26.8–26.9 to 26.7–26.8 σ_θ during these periods (Fig. 4a). As the warming signal is observed in the density range lighter than the salinity minimum, the freshening signals on these isopycnal surfaces are related to both freshening and warming signals. These freshening and warming signals in the North Pacific are consistent with the changes from 1930 to 1980 and from 1985 to 1994 along the zonal section at 24°N (Wong et al. 1999). On the other hand, the freshening signal in the salinity minimum density range is not explained only by the warming signal because of the curvature of the salinity minimum.

As an analogy of the observed change in NPIW, the observed OSIW shows a decrease in salinity and/or warming at the salinity minimum density for NPIW (Fig. 4b). However, this decrease in salinity and/or warming signal is translated to an apparent warming and salinification signal on the isopycnal surface in the Sea of Okhotsk (see also Fig. 3b) because the slopes of the observed temperature and salinity profiles are smaller than the ambient isopycnal slope, which is different from those in the western subtropical North Pacific. The OSIW basically outflows to the North Pacific along isopycnal surfaces, although some modifications occur because of the diapycnal mixing caused by strong tidal current around the Kuril Straits (Wong et al. 1998). Therefore, assuming that isopycnal mixing and advection processes are dominant on the salinity minimum density surface, the freshening signal in the downstream region (i.e., NPIW) at this density cannot be explained by advection of the apparent warmed and salinity-increased OSIW. The result that the apparent salinity-increasing signal in the source region is not found in the downstream regions implies that the freshening signal in the western subtropical North Pacific is likely to overwhelm the source water signal.

The *T*–*S* diagram obtained from the simulated data also shows that the water masses in the range of salinity minimum density averaged over the western subtropical North Pacific have been freshened and that the salinity minimum density has decreased somewhat from 26.8–26.9 to 26.7–26.8 σ_θ, which is consistent with the observed freshening behavior, although the absolute value of the simulated salinity minimum is ~1 psu higher than the observed data (Fig. 5a). Contrary to the observed data, the simulated OSIW salinity has decreased somewhat on the isopycnal surface of the salinity minimum density (Fig. 5b). However, the freshening rate is −0.0016 psu at 26.8 σ_θ, which is much smaller than that for the western subtropical North Pacific (−0.025 psu) (Table 1; Fig. 5a). Therefore, assuming that the outflow rate from the Sea of Okhotsk is constant, the simulated freshening in the NPIW is not fully explained by only the isopycnal mixing and advection processes with freshening in the source water.

5. Mechanisms for change in NPIW properties

As the model simulated the basic pattern and strength of the freshening in the salinity minimum density of NPIW, examination of the model can provide insight into the role of wind stress change on the observed freshening. In this section, we explore the possible mechanism involved by use of model datasets (such as a 50-yr record of intermediate salinity, PV, and current speed), which are not fully available in the observational record.

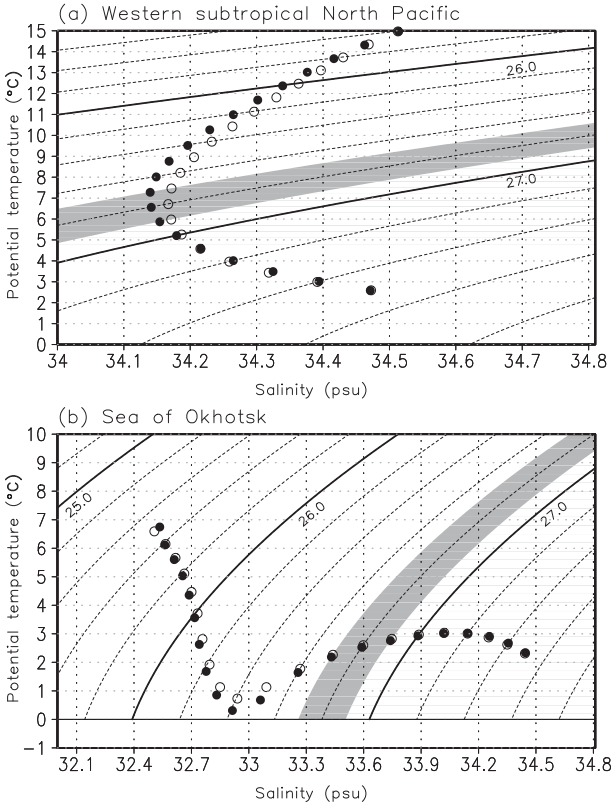

FIG. 5. As in Fig. 4, but for the simulated data.

a. *Processes of water mass property modification*

The life cycle of simulated freshening in the NPIW was investigated, as shown in Fig. 6, using a lead–lag correlation analysis of the salinity at 26.8 σ_θ and a time series of the salinity averaged over the subtropical recirculation region (22.5°–37.5°N, 135°–170°E). In this analysis, we applied a 7-yr low-pass filter to the salinity data to analyze the variability related to the multidecadal-scale freshening. The lead–lag correlation map for zero lag is shown in Fig. 6e. At a lag of −6 yr, significant positive correlations appear over the MWR southeast of Hokkaido and the recirculation of the subtropical gyre. From lags of −4 to 0 yr, the former part of the significant positive correlation develops and expands southward across the Kuroshio Extension. It then further propagates southwestward along the anticyclonic circulation of the subtropical gyre, merges with the latter part of the significant correlation at lag +4 yr, and gradually disappears at lag +6 yr. Because the latter part of the significant positive correlation is limited around the recirculation of the subtropical gyre, this signal is probably related to the westward extension of the low-salinity tongue (Nakano et al. 2005).

The rapid propagation of fresher subarctic water from the MWR to the subtropical gyre suggests that the southward transport of subarctic water cannot be explained by only frontal isopycnal mixing processes along the eastern subarctic–subtropical frontal zone (You 2003). The southward propagation of the subarctic water is in a perpendicular direction to the zonally extended geostrophic streamline associated with the Kuroshio Extension. This result suggests that mesoscale eddies and small-scale disturbances with filament-like structures are important for the southward transport of subarctic water (Mitsudera et al. 2004; Ishikawa and Ishizaki 2009).

An analysis of the simulated PV, which is an index for OSIW (Yasuda et al. 1996), indicates increases in the fraction of the OSIW present in these waters, resulting in a freshening of the MWR and the NPIW in the western Pacific subtropical gyre. The PV difference shows a significant decrease over the subtropical gyre, with the maximum in the MWR (Fig. 7), which is similar to the spatial pattern for potential temperature (Fig. 2b). This result indicates that the low-PV water, which originates in the Sea of Okhotsk, mainly contributes to the freshening of the NPIW. It is noted that the difference in the PV within the Sea of Okhotsk and near the Kuril Straits is positive, contrary to that in the NPIW. Therefore, advection of the PV anomaly in the Sea of Okhotsk is not essential for the significant decrease in PV in the MWR.

b. *Possible causes of MWR freshening: Southward Oyashio intrusion and mesoscale eddy activity*

From the time evolution of the salinity on the isopycnal surface, it was found that the water mass property change in the MWR is responsible for the freshening in the subtropical gyre. The salinity and PV on the isopycnal surface have decreased, and this indicates that the southward transport of the Oyashio water, which is characterized by low-PV water originating from the Sea of Okhotsk, has increased. As the signal of the salinity change originates from MWR and expands southward across the Kuroshio Extension, it is considered that the effects of direct Oyashio advection are limited to MWR. Here, we qualitatively examine the Oyashio along the northeast coast of Japan and the activities of mesoscale eddies in relation to the water mass property change in the MWR based on the simulated data.

Based on the annually averaged current velocity field, we first examine the southward intrusion of the Oyashio. Figures 8a and 8b compare the mean state of the current velocity at 26.8 σ_θ based on the model simulation in the former and latter periods from 1955 to 2005. Southwestward flow of the Oyashio is clearly found along the Kuril Straits, and the southward intrusion becomes relatively large in the latter decades. This difference becomes clearer in Fig. 8c, which shows a current velocity

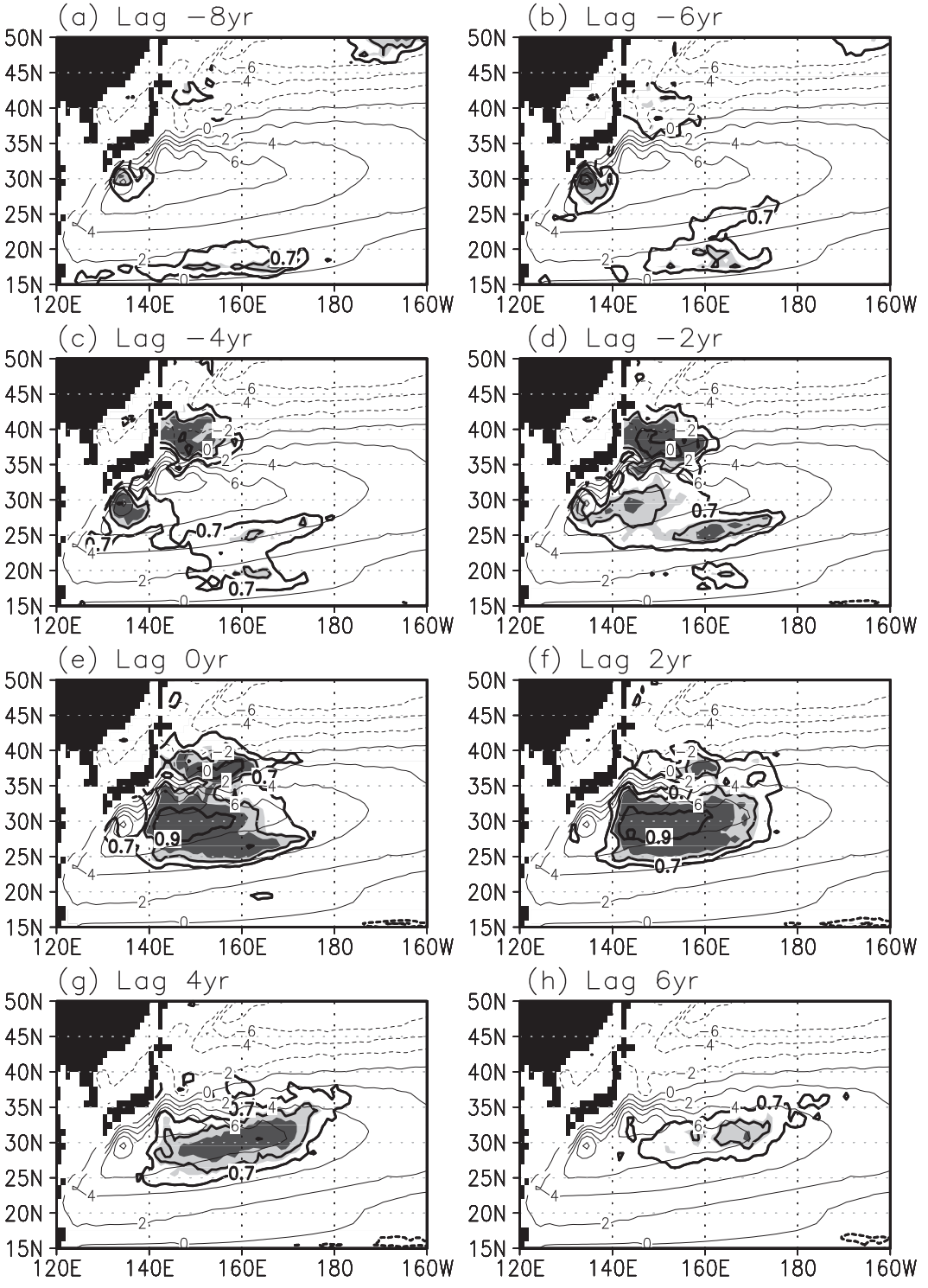

FIG. 6. Lead–lag correlation maps (thick contours) of 7-yr low-pass filtered annually averaged salinity at 26.8 σ_θ, with the time series averaged over the subtropical recirculation gyre (22.5°–37.5°N, 135°–170°E) at lags (a) −8, (b) −6, (c) −4, (d) −2, (e) 0, (f) +2, (g) +4, and (h) +6 yr. The contour interval is 0.1, and values less than 0.7 are omitted. The light and heavy shadings indicate the regions where the absolute value of the correlation is significant at the 90% and 95% confidence level, respectively. The climatology of annual-mean pressure (kPa) at 26.8 σ_θ (thin contours) is superimposed on each panel.

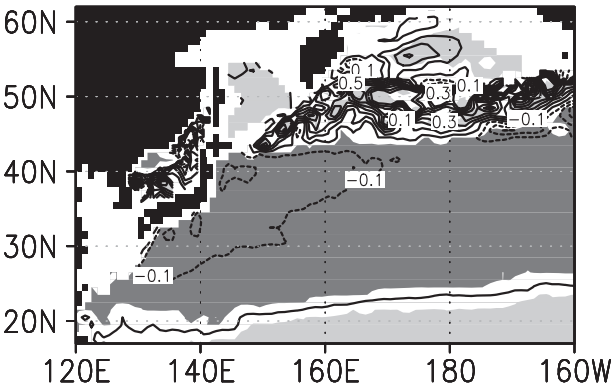

FIG. 7. Change in the annually averaged PV at 26.8 σ_θ from 1955–76 to 1977–2004 for the model simulation. The contour interval is $0.05 \times 10^{-10}\,\mathrm{m^{-1}\,s^{-1}}$. Negative values indicate that PV decreased from 1955–76 to 1977–2004. The light (heavy) shading indicates the region where the positive (negative) difference is significant at the 95% confidence level.

difference map between the latter (1977–2004) and former (1955–76) periods.

To examine the relationship between the southward volume transport of the Oyashio and salinity in the MWR on specific isopycnal surfaces, an index for the southward transport of the Oyashio (V_{oya}) is defined as follows:

$$V_{\mathrm{oya}} = -vhl_x. \tag{1}$$

Here, v is the negative meridional velocity ($\mathrm{m\,s^{-1}}$), h is the layer thickness (m) averaged over the Oyashio (42°–44°N, 147°–149°E; see Fig. 8c) on specific isopycnal surfaces, and l_x is the width of the Oyashio (m) near the southern end, which is fixed as a constant. A positive anomaly of V_{oya} means that the southward transport is strengthened relative to the climatological value. The isopycnal layer thickness is defined as the distance between ± 0.05 σ_θ on a specified isopycnal surface.

Figure 9 shows a time series of the annually averaged anomalies of V_{oya} at 26.8 σ_θ (solid line). The mean V_{oya} at 26.8 σ_θ in the former and latter 25 yr is 0.05 and 0.23 Sv, respectively. The quantity V_{oya} is characterized by the transient change in the 1970s, which is similar to the salinity anomalies (dashed line) averaged over the MWR (40°–44°N, 145°–150°E). The correlation between these is 0.54 at no time lag (significant at the 95% confidence level), indicating that the Oyashio advection directly affects the water property in MWR. The increase in V_{oya} also occurs on the surrounding isopycnal surfaces with the maximum at 26.8 σ_θ (Table 2), indicating that the southward Oyashio transport increased in the salinity minimum density range. The strengthened southward transport of the Oyashio in the 1970s is

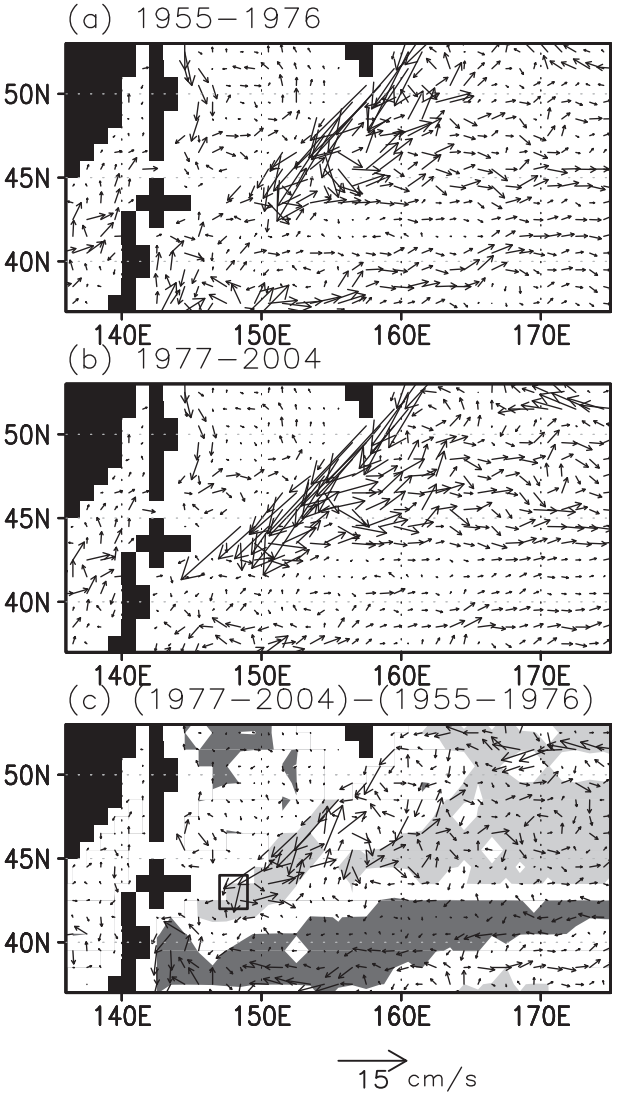

FIG. 8. The mean state of annually averaged current velocity ($\mathrm{cm\,s^{-1}}$) at 26.8 σ_θ from the model simulation: (a) 1955–76, (b) 1977–2004, and (c) the difference of the mean state between the latter (1977–2004) and former (1955–76) periods. In (c), the dense and light shades indicate regions where the negative and positive difference of the absolute current speed is significant at the 95% confidence level, respectively. For the calculation of the significance, we assume that each year is independent.

consistent with the southward transition of the Oyashio Front, as estimated from observational sea surface temperature (Yasuda 2003).

We then evaluated the effect of mesoscale eddies on the southward transport of the OSIW. As in the index of strength of the mesoscale eddies, the pseudo eddy kinetic energy (EKE) [defined as $(u^2+v^2)/2$ on the isopycnal surface] was used. To emphasize the contribution from the mesoscale eddies on the velocity field, EKE was calculated based on high-pass filtered current

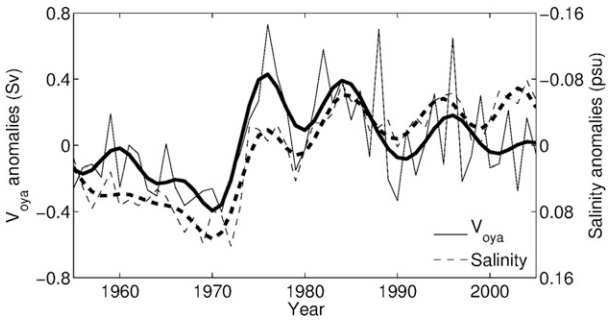

FIG. 9. Time series of annually averaged V_{oya} in the rectangular region shown in Fig. 8c (solid line) and salinity anomalies in the MWR (40°–44°N, 145°–150°E) (dashed line) at 26.8 σ_θ. The positive anomaly of V_{oya} means that the southward transport of the Oyashio is strengthened relative to the climatological value. The term V_{oya} at 26.8 σ_θ is calculated from the meridional velocity and layer thickness defined as the distance between ± 0.05 σ_θ at the corresponding isopyncal surface, as defined by Eq. (1). Thick lines denote 7-yr low-pass filtered data. Note that salinity anomalies are shown on the axis of negative upward.

velocity data with a time scale shorter than 10 months. Although EKE does not strictly include small-scale disturbances, the interpolation procedure on the full-resolution model output enabled this expression to be useful for qualitative examination of changes in the mesoscale eddies in the midlatitudes on spatial scales of around several hundred kilometers.

Figures 10a and 10b compare the mean state of EKE at 26.8 σ_θ in the former and latter 25 yr. The highest variability of EKE occurs along the Kuril Straits and at the Oyashio Front around 46°N. The difference map (Fig. 10c) showing EKE between the latter and former periods indicates a greater value of EKE in the Oyashio Front in the latter decades. Figure 11 shows time series of annually averaged EKE in the Oyashio Front over the rectangular region shown in Fig. 11c (solid line) and of annually averaged salinity (same as in Fig. 9; dashed line). The time series of EKE is characterized by an apparent change in the early 1980s. The correlation between EKE and the salinity anomalies averaged over the MWR is −0.61 (significant at the 95% confidence level) at no time lag. This also suggests enhanced cross-gyre transport in the latter period.

The enhanced cross-gyre transport at the salinity minimum density is also confirmed from the PV difference map (Fig. 7). A significant decrease in PV is observed in the subtropical gyre, but PV increased in the subarctic North Pacific. The difference map in isopycnal layer thickness at 26.8 σ_θ shows a pattern similar to that of the PV difference but with opposite sign (not shown), indicating that these PV changes are approximately explained by the change in isopycnal layer thickness. Because the volume on the salinity minimum density in the subarctic North Pacific has decreased, in contrast with the western subtropical North Pacific, it is suggested that the enhanced Oyashio transport drains the reservoir of the subarctic water.

TABLE 2. Difference of the annually averaged V_{oya} (Sv) on isopycnal surfaces between 1977–2004 and 1955–76. Bold numbers indicate the differences that exceed the 95% confidence levels based on the Student's t test.

σ_θ	26.6	26.7	26.8	26.9	27.0	27.1
ΔV_{oya}	**0.11**	**0.15**	**0.18**	**0.17**	**0.14**	**0.12**

Nakano et al. (2005) suggested a relationship between the westward extension of a low-salinity tongue along the recirculation in the subtropical gyre and salinity change in the NPIW on an interannual to decadal time scale. The model simulation showed that the significant freshening signal originates from the recirculation of the subtropical gyre (Fig. 6). We can expect, therefore, that the freshening at the salinity minimum density of NPIW is also affected by changes in the size of the low-salinity tongue, which is accompanied by freshwater on the isopycnal surface. Using correlation analysis, we briefly evaluated the effect of the subtropical gyre circulation change on the freshening in NPIW. As an index for the strength of the subtropical gyre circulation, we used the recirculation index defined by the meridional gradient of the isopycnal surface at 26.8 σ_θ between 28° and 18°N at 137°E, according to Nakano et al. (2005). The correlation map between the recirculation index and the salinity shows that a significant negative correlation occurs south of Japan (120°–140°E) (Fig. 12) and that this corresponds to the position of the climatological low-salinity tongue (in which the zonal gradient of salinity is relatively large). This result therefore indicates that the freshening of the NPIW is partly related to the westward extension of the low-salinity tongue, but the effect is limited to the southwestern part of the subtropical gyre.

c. *Basin-scale wind stress pattern related to the change in Oyashio transport*

The analysis of mean current and eddy fields suggests that intensified mesoscale eddies together with strengthened southward Oyashio transport are related to the freshening in the MWR. Previous observational and modeling studies have suggested that interannual variability of the southward Oyashio transport is related to wintertime changes in basin-scale wind stress with no time lag (Sekine 1988; Isoguchi et al. 1997; Nonaka et al. 2008). These studies have suggested that a barotropic adjustment of the ocean circulation, via westward propagation of Rossby waves, is responsible for the interannual

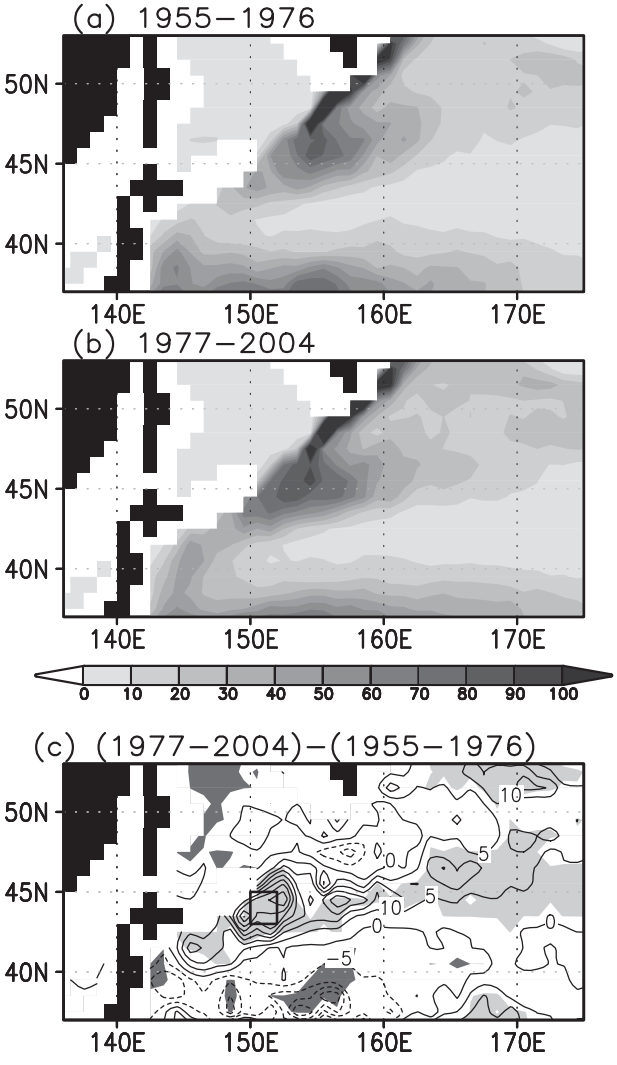

FIG. 10. The mean state of annually averaged EKC ($cm^2\,s^{-2}$) at 26.8 σ_θ from the model simulation: (a) 1955–76, (b) 1977–2004, and (c) the difference of the mean state between the latter (1977–2004) and former (1955–76) periods. In (c), the light and dense shades indicate regions where the positive and negative difference is significant at the 95% confidence level, respectively. For calculation of the significance, we assume each year is independent.

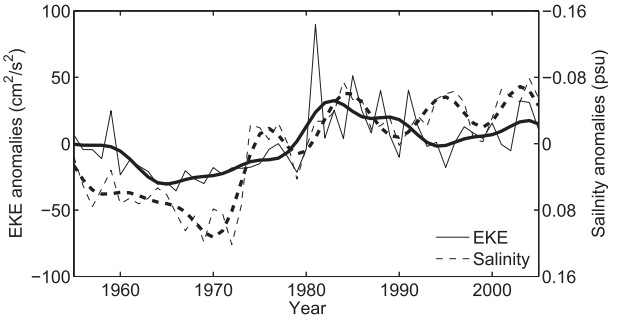

FIG. 11. The time series of annually averaged EKE anomalies in the rectangular region near the subarctic front shown in Fig. 10c (solid line) and salinity anomalies in the MWR (40°–44°N, 145°–150°E) (dashed line) at 26.8 σ_θ, as in Fig. 9. Thick lines denote 7-yr low-pass filtered data.

variability of the Oyashio in the intermediate layer. To confirm that the southward Oyashio transport can be explained by this theory on a multidecadal time scale, we examined the relationship between V_{oya} at 26.8 σ_θ and the wind stress curl in winter (December–February). As it is known that a multidecadal large-scale atmospheric variability is evident in spring (Minobe 2000), we also examined this relationship during spring (March–May).

Figure 13a shows a regression map of the wind stress curl onto the annually averaged V_{oya} at 26.8 σ_θ with a 7-yr low-pass filter in winter. The regression map demonstrates that significant basin-scale positive wind stress curl anomalies north of 45°N in the North Pacific are related to the anomalous southward transport of the Oyashio, with no time lag. The regression map of sea level pressure (Fig. 13c) indicates that the positive anomaly of the wind stress curl is related to the strengthened Aleutian low (Fig. 13c), which is similar to the basinwide scale change in SLP related to the PDO (Mantua et al. 1997; Minobe 1997). Thus, the regression pattern implies a significant intensification of the subarctic gyre related to the PDO, resulting in the anomalous southward transport of the Oyashio.

In spring, V_{oya} is also significantly correlated with the wind stress curl over the subarctic North Pacific (Fig. 13b) and the sea level pressure over the North Pacific (Fig. 13d) when the former lags the latter by 3 yr. The wind stress curl in the western subarctic gyre (~165°E) is highly correlated with V_{oya}. The distance between the western boundary and 165°E is about 1200 km at 42°N. A long baroclinic Rossby wave speed is estimated to be ~1.3 $cm\,s^{-1}$ at this latitude (Qiu 2002). Therefore, the time span of the journey is estimated to be 2.9 yr, which is comparable to the lag time between V_{oya} and the wind stress curl.

The above analyses suggest that the freshening in the NPIW is caused by intensification of the wind-driven ocean circulation in the subarctic gyre and the succeeding strengthening southward transport of OSIW to MWR. To confirm this suggestion, we examined the relationship between the strength of the atmospheric circulation over the subarctic North Pacific and the salinity of NPIW by using a historical dataset and the North Pacific index—the area-averaged sea level pressure over the region 30°–65°N, 160°E–140°W, the rectangular region shown in Fig. 11c, from December to March (Trenberth and Hurrell 1994)—from 1925 to 2004.

Figure 14a shows time series of 5-yr running-mean salinity at 26.8 σ_θ averaged over the western subtropical

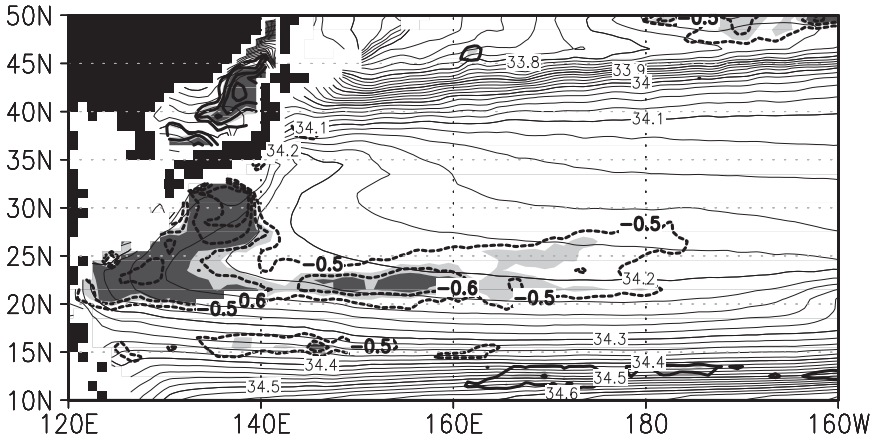

FIG. 12. Correlation maps (thick contours) of 7-yr low-pass filtered annually averaged salinity at 26.8 σ_θ, with the recirculation gyre index. The contour interval is 0.1 and values less than 0.5 are omitted. The light and heavy shades indicate regions where the absolute value of the correlation is significant at the 90% and 95% confidence level, respectively. The annual climatology of salinity (thin contours) at 26.8 σ_θ is superimposed.

gyre and the NPI. Both time series are dominated by interdecadal variability. From 1925 to 2004, the lead–lag correlation between these indicates that the maximum positive correlation (larger than 0.44, significant at the 90% confidence level) is found when the NPI leads the salinity by 7 to 8 yr, as shown in Fig. 14b. This time lag is comparable to the sum of the time lag between the Oyashio transport and the wind stress curl over the subarctic North Pacific of 0–3 yr, as shown in Fig. 13, and the time lag between the salinity anomalies in the MWR and

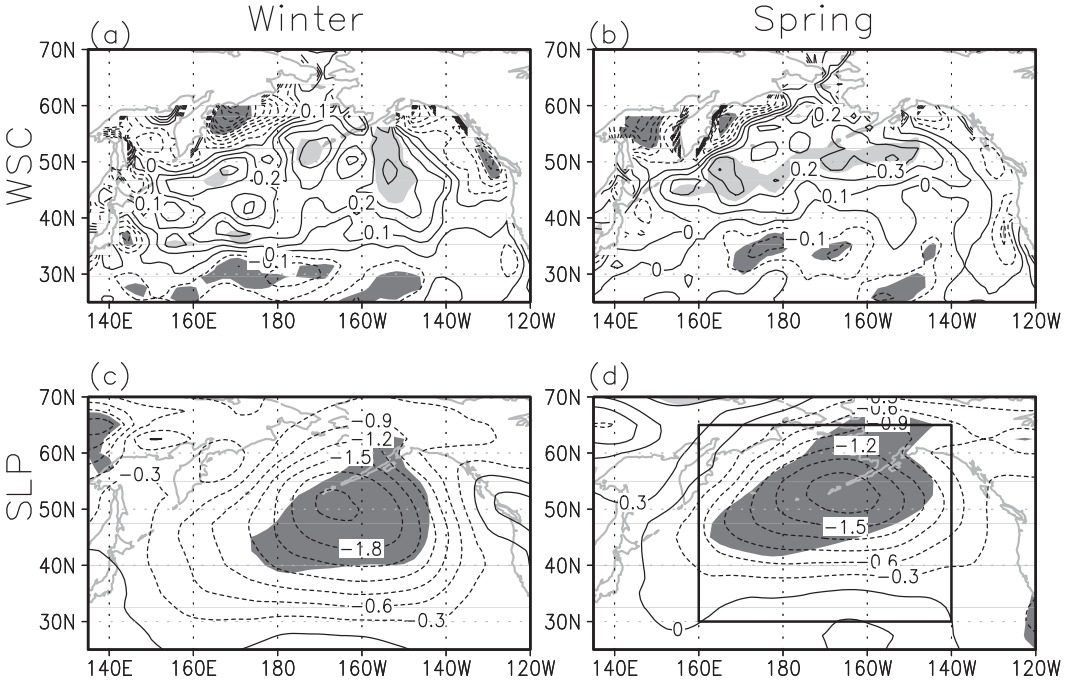

FIG. 13. Regression maps of annually averaged (a),(b) wind stress curl and (c),(d) sea level pressure in (left) winter and (right) spring onto the normalized time series of annually averaged V_{oya} at 26.8 σ_θ with a 7-yr low-pass filter. In the left and right panels, V_{oya} leads the wind stress curl and sea level pressure fields by 0 and 3 yr. The contour interval is (top) 0.1×10^{-7} N m^{-3} and (bottom) 0.3 hPa. The light and heavy shades indicate regions where the positive and negative correlation is significant at the 90% confidence level, respectively. In (d), the boundary for the calculation of NPI is indicated.

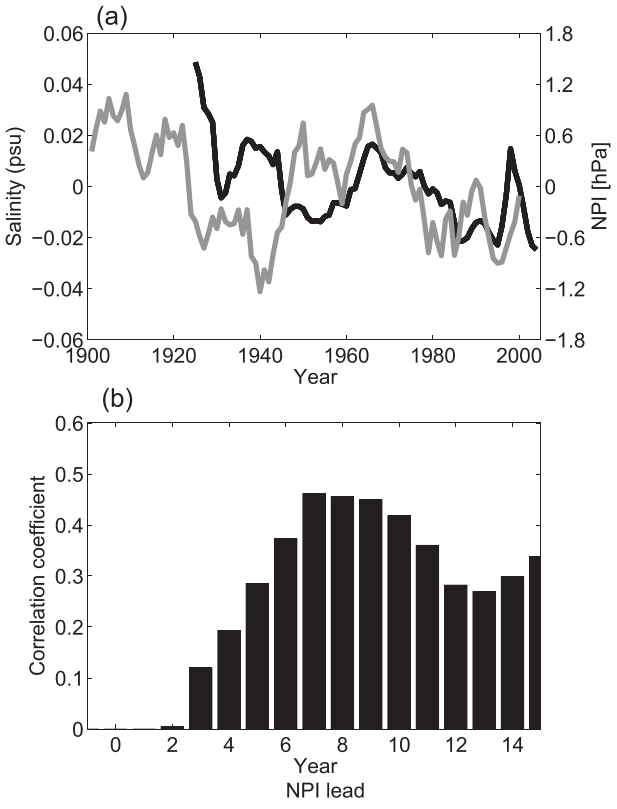

FIG. 14. (a) Time series of the 5-yr running mean of annual-mean salinity anomalies at 26.8 σ_θ averaged over the western subtropical North Pacific (rectangular region denoted by purple lines in Fig. 2a) (black) and NPI anomalies (gray) from December to the following May. The scale of the NPI is indicated on the right axis. (b) Lead–lag correlations between the 5-yr running mean of salinity at 26.8 σ_θ and the NPI from 1925 to 2004.

the subtropical recirculation gyre of 6 yr, as shown in Fig. 7. These results strongly support the idea that multidecadal-scale intensification in Aleutian low wind stress over the subarctic gyre in the North Pacific largely contributes to the freshening in the NPIW through the strengthened southward transport of the OSIW.

6. Summary and discussion

Wong et al. (1999, 2001) reported that between the 1960s and 1990s, significant freshening from surface to intermediate depths occurred in the North Pacific. They suggested that the observed changes in salinity of NPIW could be interpreted as the result of an increase in the freshwater flux over the source region and, along with the other hydrographic sections in this study, are consistent with an increase in Earth's hydrological cycle. On the other hand, a half-century scale change characterized by the deepened Aleutian low of 1977/78 (Nitta and Yamada 1989; Trenberth 1990), which is known to be a part of the periodic change of the PDO (Mantua et al. 1997; Minobe 1997), is an alternative interpretation for the freshening in NPIW because the southward transport of the Oyashio water can be governed by large-scale wind stress change (Sekine 1988; Isoguchi et al. 1997; Nonaka et al. 2008). In this study, we used all available historical oceanographic data and model simulation of an eddy-resolving ice–ocean coupled model to examine the spatial pattern of the multidecadal-scale change in the NPIW and the role of the wind-driven ocean circulation change with emphasis on the salinity minimum density.

From historical observations, it was found that the salinity at the salinity minimum density of NPIW (26.8 σ_θ), which does not outcrop in the North Pacific, decreased significantly in the western subtropical gyre from 1955 to 2004. The freshening was characterized by the transient change apparent in the late 1970s. Although the observed OSIW also shows freshening and/or warming at the salinity minimum density for NPIW (as shown in Fig. 2 and the previous studies; e.g., Nakanowatari et al. 2007), this freshening and/or warming signal is translated to an apparent warming and salinification signal on the isopycnal surface in the Sea of Okhotsk. Therefore, assuming that advection and mixing processes are dominant on the isopycnal surface, this observational evidence does not support the hypothesis that freshening in the source water is essential for the freshening in NPIW at this density.

To evaluate the effect of the change in the wind-driven ocean circulation, a model experiment, in which the wind stress was varied interannually but the SSS was restored to the climatological value, was performed. The observed freshening in the western part of NPIW was basically simulated in the model output. The freshening is at a maximum in the MWR and is accompanied by a decrease in PV. A lead–lag correlation analysis indicated that the freshening signal is advected southward across the Kuroshio Extension, where it then travels along the recirculation of the subtropical gyre. This result demonstrates that the freshening is not simply related to the southward shift of the subarctic front (Joyce and Dunworth-Baker 2003) but also to advection of subarctic water (which is mainly supplied from the Sea of Okhotsk) into the subtropical gyre. In addition, the advection time of the freshening signal between the MWR and the recirculation gyre region is 6 to 9 yr, which is 2 times shorter than the advection time of the subtropical gyre circulation (You 2003). These results support the idea that the eddy-driven shortcut pathway of the OSIW, clarified by observational (Yasuda et al. 1996) and numerical (Mitsudera et al. 2004; Fujii et al. 2013) studies, is likely affecting the multidecadal-scale freshening in NPIW.

With respect to the physical processes involved in the advection of OSIW to the MWR, we examined the

strength of the southward transport of the Oyashio and mesoscale eddies. The model outputs showed that both the Oyashio and the mesoscale eddies strengthened in the late 1970s, suggesting that both mechanisms are related to the increase in southward transport of the Oyashio water. Recently, Fujii et al. (2013), based on the tangent linear and adjoint models, clarified that a large fraction of the low-salinity-origin water of NPIW, which comes from the Sea of Okhotsk, is advected to the MWR by the Oyashio and then enters the subtropical gyre. This study supports the suggestion that Oyashio water entering the MWR, which increased in the late 1970s, is effectively transported south of the KE along the region east of Japan.

For the strengthened mesoscale eddy activity, there is a possibility that the baroclinicity along the Oyashio Front is intensified by the changes in the Oyashio. This speculation is consistent with an earlier study (Garnier and Schopp 1999) in which mesoscale eddy activity was shown to be strengthened along the frontal regions of the Gulf Stream and the North Atlantic Current when these currents increase. Therefore, such a process may affect the multidecadal-scale change in mesoscale eddy activity near the Oyashio Front.

On the other hand, the center of freshening in the model is north of the Kuroshio Extension (the strongest freshening is found in the MWR), which is different from that in the observations (south of the Kuroshio Extension). Because the simulated change in the area-averaged salinity over the western subtropical gyre south of the Oyashio Front is comparable to the observed value, the simulated Oyashio water entering the MWR may not fully be transported farther southward across the KE by mesoscale and/or submesoscale eddies. In a mean state, the southward transport of Oyashio water across 40°N, west of 150°E in our simulation, is less than the value based on the observational data (Ishikawa and Ishizaki 2009). The lead–lag correlation analysis demonstrated that the multidecadal anomaly originating from the MWR is qualitatively advected to the subtropical gyre across the KE, but its amount may be underestimated. For a quantitative analysis of the contribution of the Oyashio and mesoscale eddies to the freshening in the NPIW, a study based on a model further improved with respect to the representation of mesoscale eddies in and around the KE is needed.

The multidecadal change in the Oyashio is also accompanied by a strengthened wind stress curl over the subarctic North Pacific. As the strengthened wind stress curl is characterized by the deepening of the Aleutian low, the southward transport of Oyashio water is possibly related to the 1976/77 regime shift, which is part of the PDO. To date, a response of the surface and subsurface water temperature in the central and western North Pacific to the 1976/77 regime shift has been reported (Deser et al. 1996; Yasuda and Hanawa 1997). The resultant cooler surface waters subducted into the main thermocline and propagated southwestward as anomalies of thermocline depth (Schneider et al. 1999; Tourre et al. 1999). Wind anomalies over the central North Pacific also caused the midlatitude gyre change, which resulted in the subsurface water temperature anomalies in the Kuroshio–Oyashio Extension (KOE) region (Miller et al. 1998; Deser et al. 1999). However, these earlier studies focused on the responses of surface and/or subsurface water temperature to the 1976/77 regime shift with emphasis on the subtropical gyre change. Our study suggests the importance of the change in the subarctic gyre and the related southward Oyashio transport on the multidecadal-scale freshening in the NPIW at the salinity minimum density.

Thus, it is suggested that wind-driven cross-gyre transport through the MWR is the likely cause for the multidecadal-scale freshening signal at the salinity minimum density of NPIW, as summarized in the schematics of Fig. 15. Before the 1976/77 regime shift (top panel in Fig. 15), the Oyashio water, which was modified by OSIW, was transported to MWR across the Oyashio Front (broken blue line in Fig. 15). The subarctic water was further transported to the subtropical gyre across KE (broken red line in Fig. 15) by eastward current and mesoscale eddies. After the regime shift (Fig. 15b), the subarctic gyre strengthened and the southward transport of Oyashio water across the Oyashio Front was also intensified by the Oyashio transport and mesoscale eddies, resulting in freshening in MWR. The freshened water in MWR was quickly advected to the subtropical gyre by mesoscale eddies across KE. Although heat and salt contents are not changed within the entire North Pacific basin, the wind-driven cross-gyre transport of the subarctic water may be important for the redistribution of heat and freshwater.

In the model simulation, the sea surface salinity was restored to the climatological value, although the freshwater fluxes are time varying. Because thermohaline effects were not adequately represented in this simulation, our experiment could not exclude the possibility of surface freshening affecting the freshening in NPIW at densities lighter than 26.5 σ_θ, the source water of which outcrops in the Gulf of Alaska (Wong et al. 1999, 2001). In fact, the change in SSS shows a significant decrease in this region (Durack and Wijffels 2010). On the other hand, we emphasize that the low-salinity water advection influenced the long-term salinity change in the western subtropical gyre. The volume on the salinity minimum density has increased (decreased) in the

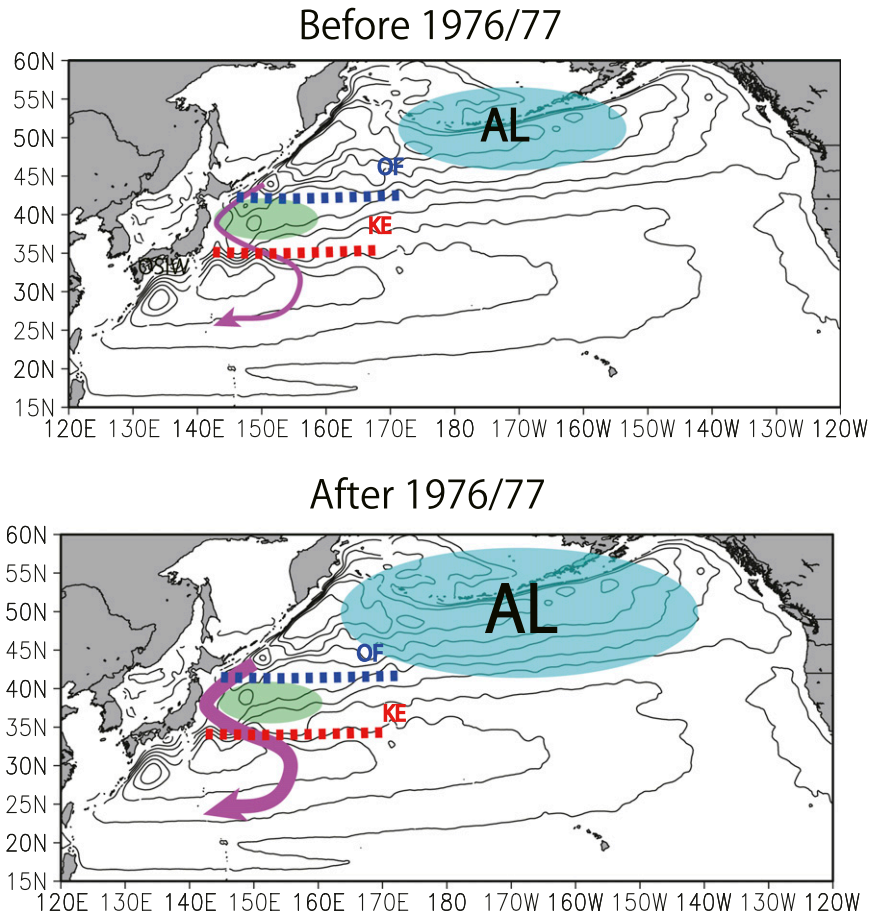

FIG. 15. Schematic of the freshening processes at the salinity minimum density of NPIW, driven by the 1976/77 regime shift in the wind stress.

western subtropical (subarctic) North Pacific, indicating that the enhanced Oyashio transport drains the reservoir of the subarctic water. Thus, there is a need to exactly estimate long-term freshwater input changes in consideration of the lateral advection process.

The observed warming of OSIW reported by earlier studies, which is translated to a salinification signal on the isopycnal surface, was not reproduced in our model experiment (Figs. 2b, 3b). Because the simulated SSS was restored to the climatological value, the absence of the warming signal in the simulated data may be related to the fact that the effect of interannual variation in thermodynamic processes in the Sea of Okhotsk was not well represented in this model simulation. This result is consistent with earlier studies, in which significant effects of air temperature variability over the Sea of Okhotsk on ocean temperature at intermediate depths have been shown by observed data (Kashiwase et al. 2014) and model simulations (Matsuda et al. 2009; Fujisaki et al. 2011; Nakanowatari et al. 2014) through sea ice production. Furthermore, earlier studies have reported a significant freshening signal in the upper intermediate layer of the Sea of Okhotsk (Hill et al. 2003; Ohshima et al. 2014). The analysis of the *T*–*S* properties of OSIW supports that the increase in the observed salinity of OSIW on the isopycnal surface can be explained by both warming and freshening signals. Therefore, model experiments including thermodynamic processes and diagnostic analysis of the *T*–*S* curve (Bindoff and McDougall 1994, 2000) are needed to quantitatively examine the cause for the salinity increase signal on the isopycnal surface in OSIW.

Acknowledgments. The Argo float data used in this study were collected and made freely available by the International Argo Project and the national programs that contribute to it. Part of the hydrographic data in the Okhotsk Sea was obtained in cooperation with the Far Eastern Regional Hydrometeorological Research Institute, Scripps Institute of Oceanography, and S. C. Riser of University of Washington. We thank Dr. G. Williams for carefully proofreading our manuscript. The model

simulation and hydrographical data were analyzed on the Pan–Okhotsk Information System of ILTS. We thank three anonymous reviewers for their constructive comments. Some figures were produced with the GrADS package developed by B. Doty. This work was supported by a Grand-in-Aid for Scientific Research (19340131 and 22221001) and Scientific Research on Innovative Areas (22106010) and by a fund from the Core Research for Evolution Science and Technology (CREST), Japan Science and Technology Corporation (JST).

REFERENCES

Andreev, A., and S. Watanabe, 2002: Temporal changes in dissolved oxygen of the intermediate water in the subarctic North Pacific. *Geophys. Res. Lett.,* **29,** 1680, doi:10.1029/2002GL015021.

Antonov, J., S. Levitus, T. P. Boyer, M. Conkright, T. O'Brien, and C. Stephens, 1998: *Temperature of the Pacific Ocean.* Vol. 2, *World Ocean Atlas 1998,* NOAA Atlas NESDIS 28, 166 pp.

Auad, G., J. P. Kennett, and A. J. Miller, 2003: North Pacific Intermediate Water response to a modern climate warming shift. *J. Geophys. Res.,* **108,** 3349, doi:10.1029/2003JC001987.

Bindoff, N. L., and T. J. McDougall, 1994: Diagnosing climate change and ocean ventilation using hydrographic data. *J. Phys. Oceanogr.,* **24,** 1137–1152, doi:10.1175/1520-0485(1994)024<1137:DCCAOV>2.0.CO;2.

——, and ——, 2000: Decadal changes along an Indian Ocean section at 32°S and their interpretation. *J. Phys. Oceanogr.,* **30,** 1207–1222, doi:10.1175/1520-0485(2000)030<1207:DCAAIO>2.0.CO;2.

Bond, N. A., J. E. Overland, M. Spillance, and P. Stabeno, 2003: Recent shifts in the state of the North Pacific. *Geophys. Res. Lett.,* **30,** 2183, doi:10.1029/2003GL018597.

Boyer, T. P., S. Levitus, J. Antonov, M. Conkright, T. O'Brien, and C. Stephens, 1998: *Salinity of the Pacific Ocean.* Vol. 5, *World Ocean Atlas 1998,* NOAA Atlas NESDIS 31, 166 pp.

Conkright, M. E., and Coauthors, 2002: *Introduction.* Vol. 1, *World Ocean Database 2001,* NOAA Atlas NESDIS 42, 167 pp.

Deser, C., M. A. Alexander, and M. S. Timlin, 1996: Upper-ocean thermal variations in the North Pacific during 1970–1991. *J. Climate,* **9,** 1840–1855, doi:10.1175/1520-0442(1996)009<1840:UOTVIT>2.0.CO;2.

——, ——, and ——, 1999: Evidence for a wind-driven intensification of the Kuroshio Current Extension from the 1970s to the 1980s. *J. Climate,* **12,** 1697–1706, doi:10.1175/1520-0442(1999)012<1697:EFAWDI>2.0.CO;2.

Durack, P. J., and S. E. Wijffels, 2010: Fifty-year trends in global ocean salinities and their relationship to broad-scale warming. *J. Climate,* **23,** 4342–4362, doi:10.1175/2010JCLI3377.1.

Emerson, S., Y. W. Watanabe, T. Ono, and S. Mecking, 2004: Temporal trends in apparent oxygen utilization in the upper pycnocline of the North Pacific: 1980–2000. *J. Oceanogr.,* **60,** 139–147, doi:10.1023/B:JOCE.0000038323.62130.a0.

Fujii, Y., T. Nakano, N. Usui, S. Matsumoto, H. Tsujino, and M. Kamachi, 2013: Pathways of the North Pacific Intermediate Water identified through the tangent linear and adjoint models of an ocean general circulation model. *J. Geophys. Res. Oceans,* **118,** 2035–2051, doi:10.1002/jgrc.20094.

Fujisaki, A., H. Mitsudera, and H. Yamaguchi, 2011: Dense shelf water formation process in the Sea of Okhotsk based on an ice-ocean coupled model. *J. Geophys. Res.,* **116,** C03005, doi:10.1029/2009JC006007.

Garnier, V., and R. Schopp, 1999: Wind influence on the mesoscale activity along the Gulf Stream and the North Atlantic Currents. *J. Geophys. Res.,* **104,** 18 087–18 110, doi:10.1029/1999JC900070.

Hill, K. L., A. J. Weaver, H. J. Freeland, and A. Bychkov, 2003: Evidence of change in the Sea of Okhotsk: Implications for the North Pacific. *Atmos.–Ocean,* **41,** 49–63, doi:10.3137/ao.410104.

Hunke, E. C., and J. K. Ducowicz, 1997: An elastic–viscous–plastic model for sea ice dynamics. *J. Phys. Oceanogr.,* **27,** 1849–1867, doi:10.1175/1520-0485(1997)027<1849:AEVPMF>2.0.CO;2.

Ishikawa, I., and H. Ishizaki, 2009: Importance of eddy representation for modeling the intermediate salinity minimum in the North Pacific: Comparison between eddy-resolving and eddy-permitting models. *J. Oceanogr.,* **65,** 407–426, doi:10.1007/s10872-009-0036-6.

Isoguchi, O., H. Kawamura, and T. Kono, 1997: A study on wind-driven circulation in the subarctic North Pacific using TOPEX/POSEIDON altimeter data. *J. Geophys. Res.,* **102,** 12 457–12 468, doi:10.1029/97JC00447.

Itoh, M., 2007: Warming of intermediate water in the Sea of Okhotsk since the 1950. *J. Oceanogr.,* **63,** 637–641, doi:10.1007/s10872-007-0056-z.

——, K. I. Ohshima, and M. Wakatsuchi, 2003: Distribution and formation of Okhotsk Sea Intermediate Water: An analysis of isopycnal climatological data. *J. Geophys. Res.,* **108,** 3258, doi:10.1029/2002JC001590.

Joyce, T. M., and J. Dunworth-Baker, 2003: Long-term hydrographic variability in the Northwest Pacific Ocean. *Geophys. Res. Lett.,* **30,** 1043, doi:10.1029/2002GL015225.

Kalnay, E. M., and Coauthors, 1996: The NCEP/NCAR 40-Year Reanalysis Project. *Bull. Amer. Meteor. Soc.,* **77,** 437–472, doi:10.1175/1520-0477(1996)077<0437:TNYRP>2.0.CO;2.

Kanamitsu, M., W. Ebisuzaki, J. Woollen, S. K. Yang, J. J. Hnilo, M. Fiorino, and G. L. Potter, 2002: NCEP–DOE AMIP-II Reanalysis (R-2). *Bull. Amer. Meteor. Soc.,* **83,** 1631–1643, doi:10.1175/BAMS-83-11-1631.

Kashiwase, H., K. I. Ohshima, and S. Nihashi, 2014: Long-term variation in sea ice production and its relation to the intermediate water in the Sea of Okhotsk. *Prog. Oceanogr.,* **126,** 21–32, doi:10.1016/j.pocean.2014.05.004.

Kouketsu, S., I. Yasuda, and Y. Hiroe, 2005: Observation of frontal waves and associated salinity minimum formation along the Kuroshio Extension. *J. Geophys. Res.,* **110,** C08011, doi:10.1029/2004JC002862.

——, I. Kaneko, T. Kawano, H. Uchida, T. Doi, and M. Fukasawa, 2007: Changes of North Pacific Intermediate Water properties in the subtropical gyre. *Geophys. Res. Lett.,* **34,** L02605, doi:10.1029/2006GL028499.

——, M. Fukasawa, D. Sasano, Y. Kumamoto, T. Kawano, H. Uchida, and T. Doi, 2010: Changes in water properties around North Pacific Intermediate Water between the 1980s, 1990s and 2000s. *Deep-Sea Res. II,* **57,** 1177–1187, doi:10.1016/j.dsr2.2009.12.007.

Levitus, S., and T. Boyer, 1994: *Temperature.* Vol. 4, *World Ocean Atlas 1994,* NOAA Atlas NESDIS 4, 150 pp.

Mantua, N. J., S. R. Hare, Y. Zhang, J. M. Wallace, and R. C. Francis, 1997: A Pacific interdecadal climate oscillation with impacts on salmon production. *Bull. Amer. Meteor. Soc.,* **78,** 1069–1079, doi:10.1175/1520-0477(1997)078<1069:APICOW>2.0.CO;2.

Masujima, M., I. Yasuda, Y. Hiroe, and T. Watanabe, 2003: Transport of Oyashio water across the Subarctic Front into the

mixed water region and formation of NPIW. *J. Oceanogr.,* **59,** 855–869, doi:10.1023/B:JOCE.0000009576.09079.f5.

Matsuda, J., H. Mitsudera, T. Nakamura, K. Uchimoto, T. Nakanowatari, and N. Ebuchi, 2009: Wind and buoyancy driven intermediate-layer overturning in the Sea of Okhotsk. *Deep-Sea Res. I,* **56,** 1401–1418, doi:10.1016/j.dsr.2009.04.014.

Mellor, G. L., and L. Kantha, 1989: An ice-ocean coupled model. *J. Geophys. Res.,* **94,** 10 937–10 954, doi:10.1029/JC094iC08p10937.

Miller, A. J., D. R. Cayan, and W. B. White, 1998: A westward-intensified decadal change in the North Pacific thermocline and gyre-scale circulation. *J. Climate,* **11,** 3112–3127, doi:10.1175/1520-0442(1998)011<3112:AWIDCI>2.0.CO;2.

Minobe, S., 1997: A 50–70 year climatic oscillation over the North Pacific and North America. *Geophys. Res. Lett.,* **24,** 683–686, doi:10.1029/97GL00504.

——, 2000: Spatio-temporal structure of the pentadecadal variability over the North Pacific. *Prog. Oceanogr.,* **47,** 381–408, doi:10.1016/S0079-6611(00)00042-2.

Mitsudera, H., B. Taguchi, Y. Yoshikawa, H. Nakamura, T. Waseda, and T. Qu, 2004: Numerical study of the Oyashio water pathways in the Kuroshio–Oyashio confluence. *J. Phys. Oceanogr.,* **34,** 1174–1196, doi:10.1175/1520-0485(2004)034<1174:NSOTOW>2.0.CO;2.

Mizuta, G., Y. Fukamachi, K. I. Ohshima, and M. Wakatsuchi, 2003: Structure and seasonal variability of the East Sakhalin Current. *J. Phys. Oceanogr.,* **33,** 2430–2445, doi:10.1175/1520-0485(2003)033<2430:SASVOT>2.0.CO;2.

Nakamura, T., T. Toyoda, Y. Ishikawa, and T. Awaji, 2006: Effects of tidal mixing at the Kuril Straits on North Pacific ventilation: Adjustment of the intermediate layer revealed from numerical experiments. *J. Geophys. Res.,* **111,** C04003, doi:10.1029/2005JC003142.

Nakano, T., I. Kaneko, M. Endoh, and M. Kamachi, 2005: Interannual and decadal variabilities of NPIW salinity minimum core observed along JMA's hydrographic repeat sections. *J. Oceanogr.,* **61,** 681–697, doi:10.1007/s10872-005-0076-5.

——, ——, T. Soga, H. Tsujino, T. Yasuda, H. Ishizaki, and M. Kamachi, 2007: Mid-depth freshening in the North Pacific subtropical gyre observed along the JMA repeat and WOCE hydrographic sections. *Geophys. Res. Lett.,* **34,** L23608, doi:10.1029/2007GL031433.

Nakanowatari, T., K. I. Ohshima, and M. Wakatsuchi, 2007: Warming and oxygen decrease of intermediate water in the northwestern North Pacific, originating from the Sea of Okhotsk, 1995–2004. *Geophys. Res. Lett.,* **34,** L04602, doi:10.1029/2006GL028243.

——, H. Mitsudera, T. Motoi, K. I. Ohshima, and I. Ishikawa, 2010: 50-yr scale cooling in North Pacific Intermediate Water simulated by eddy resolving ice-ocean coupled model (in Japanese with English abstract and figure captions). *Umi Sora,* **85,** 141–150.

——, and Coauthors, 2014: Causes of the multidecadal-scale warming of the intermediate water in the Okhotsk Sea and western subarctic North Pacific. *J. Climate,* **28,** 714–736, doi:10.1175/JCLI-D-14-00172.1.

Nishioka, J., and Coauthors, 2007: Iron supply to the western subarctic Pacific: Importance of iron export from the Sea of Okhotsk. *J. Geophys. Res.,* **112,** C10012, doi:10.1029/2006JC004055.

Nitta, T., and S. Yamada, 1989: Recent warming of tropical sea surface temperature and its relationship to the Northern Hemisphere circulation. *J. Meteor. Soc. Japan,* **67,** 375–383.

Nonaka, M., H. Nakamura, Y. Tanimoto, T. Kagimoto, and H. Sasaki, 2008: Interannual-to-decadal variability in the Oyashio Current and its influence on temperature in the subarctic frontal zone: An eddy-resolving OGCM simulation. *J. Climate,* **21,** 6283–6303, doi:10.1175/2008JCLI2294.1.

Ohshima, K. I., T. Nakanowatari, S. Riser, Y. N. Volkov, and M. Wakatsuchi, 2014: Freshening and dense shelf water reduction in the Okhotsk Sea, linked with sea ice decline. *Prog. Oceanogr.,* **126,** 71–79, doi:10.1016/j.pocean.2014.04.020.

Ono, T., T. Midorikawa, Y. W. Watanabe, K. Tadokoro, and T. Saino, 2001: Temporal increases of phosphate and apparent oxygen utilization in the surface waters of western subarctic Pacific from 1968 to 1998. *Geophys. Res. Lett.,* **28,** 3285–3288, doi:10.1029/2001GL012948.

Qiu, B., 2002: Large-scale variability in the midlatitude subtropical and subpolar North Pacific Ocean: Observations and causes. *J. Phys. Oceanogr.,* **32,** 353–375, doi:10.1175/1520-0485(2002)032<0353:LSVITM>2.0.CO;2.

Reid, J. L., Jr., 1965: *Intermediate Waters of the Pacific Ocean.* Johns Hopkins Press, 85 pp.

Sarmiento, J. L., N. Gruber, M. A. Brzezinski, and J. P. Dunne, 2004: High latitude controls of thermocline nutrients and low latitude biological productivity. *Nature,* **427,** 56–60, doi:10.1038/nature02127.

Schneider, N., A. J. Miller, M. A. Alexander, and C. Deser, 1999: Subduction of decadal North Pacific temperature anomalies: Observations and dynamics. *J. Phys. Oceanogr.,* **29,** 1056–1070, doi:10.1175/1520-0485(1999)029<1056:SODNPT>2.0.CO;2.

Sekine, Y., 1988: Anomalous southward intrusion of the Oyashio east of Japan: 1. Influence of the interannual and seasonal variations in the wind stress over the North Pacific. *J. Geophys. Res.,* **93,** 2247–2277, doi:10.1029/JC093iC03p02247.

Shcherbina, A. Y., L. D. Talley, and D. L. Rudnick, 2003: Direct observations of North Pacific ventilation: Brine rejection in the Okhotsk Sea. *Science,* **302,** 1952–1955, doi:10.1126/science.1088692.

Shimizu, Y., I. Yasuda, K. Okuda, K. Hanawa, and S. Ito, 2003: ADCP-referenced Kuroshio and Oyashio water transports for North Pacific Intermediate Water formation. *J. Phys. Oceanogr.,* **33,** 220–233, doi:10.1175/1520-0485(2003)033<0220:ARKAOW>2.0.CO;2.

St. Laurent, L. C., H. L. Simmons, and S. R. Jayne, 2002: Estimating tidally driven mixing in the deep ocean. *Geophys. Res. Lett.,* **29,** 2106, doi:10.1029/2002GL015633.

Sverdrup, H. M., W. Johnson, and R. H. Fleming, 1942: *The Oceans, Their Physics, Chemistry, and General Biology.* Prentice-Hall, 1087 pp.

Talley, L. D., 1991: An Okhotsk Sea water anomaly: Implications for ventilation in the North Pacific. *Deep-Sea Res.,* **38A,** S171–S190, doi:10.1016/S0198-0149(12)80009-4.

——, 1993: Distribution and formation of North Pacific Intermediate Water. *J. Phys. Oceanogr.,* **23,** 517–537, doi:10.1175/1520-0485(1993)023<0517:DAFONP>2.0.CO;2.

——, 2003: Shallow, intermediate, and deep overturning components of the global heat budget. *J. Phys. Oceanogr.,* **33,** 530–560, doi:10.1175/1520-0485(2003)033<0530:SIADOC>2.0.CO;2.

——, 2008: Freshwater transport estimates and the global overturning circulation: Shallow, deep and throughflow components. *Prog. Oceanogr.,* **78,** 257–303, doi:10.1016/j.pocean.2008.05.001.

——, and Y. Nagata, 1995: The Okhotsk Sea and Oyashio region. PICES Scientific Rep. 2, 227 pp.

——, and J.-Y. Yun, 2001: The role of cabbeling and double diffusion in setting the density of the North Pacific Intermediate Water salinity minimum. *J. Phys. Oceanogr.,* **31,** 1538–1549, doi:10.1175/1520-0485(2001)031<1538:TROCAD>2.0.CO;2.

Tanaka, Y., T. Hibiya, and Y. Niwa, 2010: Assessment of the effects of tidal mixing in the Kuril Straits on the formation of the North Pacific Intermediate Water. *J. Phys. Oceanogr.,* **40,** 2569–2574, doi:10.1175/2010JPO4506.1.

Tourre, Y. M., Y. Kushnir, and W. B. White, 1999: Evolution of interdecadal variability in sea level pressure, sea surface temperature, and upper ocean temperature over the Pacific Ocean. *J. Phys. Oceanogr.,* **29,** 1528–1541, doi:10.1175/1520-0485(1999)029<1528:EOIVIS>2.0.CO;2.

Trenberth, K. E., 1990: Recent observed interdecadal climate changes in the Northern Hemisphere. *Bull. Amer. Meteor. Soc.,* **71,** 988–993, doi:10.1175/1520-0477(1990)071<0988:ROICCI>2.0.CO;2.

——, and J. W. Hurrell, 1994: Decadal atmosphere-ocean variations in the Pacific. *Climate Dyn.,* **9,** 303–319, doi:10.1007/BF00204745.

Van Scoy, K. A., D. B. Olson, and R. A. Fine, 1991: Ventilation of North Pacific Intermediate Waters: The role of the Alaskan Gyre. *J. Geophys. Res.,* **96,** 16 801–16 810, doi:10.1029/91JC01783.

Wong, A. P. S., N. L. Bindoff, and J. A. Church, 1999: Large-scale freshening of intermediate waters in the Pacific and Indian Oceans. *Nature,* **400,** 440–443, doi:10.1038/22733.

——, ——, and ——, 2001: Freshwater and heat changes in the North and South Pacific Oceans between the 1960s and 1985–94. *J. Climate,* **14,** 1613–1633, doi:10.1175/1520-0442(2001)014<1613:FAHCIT>2.0.CO;2.

Wong, C. S., R. J. Matear, H. J. Freeland, F. A. Whitney, and A. S. Bychkov, 1998: WOCE line P1W in the Sea of Okhotsk: 2. CFCs and the formation rate of intermediate water. *J. Geophys. Res.,* **103,** 15 625–15 642, doi:10.1029/98JC01008.

Yasuda, I., 1997: The origin of the North Pacific Intermediate Water. *J. Geophys. Res.,* **102,** 893–910, doi:10.1029/96JC02938.

——, 2003: Hydrographic structure and variability in the Kuroshio-Oyashio transition area. *J. Oceanogr.,* **59,** 389–402, doi:10.1023/A:1025580313836.

——, K. Okuda, and Y. Shimizu, 1996: Distribution and formation of North Pacific Intermediate Water in the Kuroshio–Oyashio interfrontal zone. *J. Phys. Oceanogr.,* **26,** 448–465, doi:10.1175/1520-0485(1996)026<0448:DAMONP>2.0.CO;2.

——, S. Kouketsu, K. Katsumata, and M. Ohiwa, 2002: Influence of Okhotsk Sea Intermediate Water on the Oyashio and North Pacific Intermediate Water. *J. Geophys. Res.,* **107,** 3237, doi:10.1029/2001JC001037.

——, S. Osahune, and H. Tatebe, 2006: Possible explanation linking 18.6-year period nodal tidal cycle with bi-decadal variations of ocean and climate in the North Pacific. *Geophys. Res. Lett.,* **33,** L08606, doi:10.1029/2005GL025237.

Yasuda, T., and K. Hanawa, 1997: Decadal changes in the mode waters in the midlatitude North Pacific. *J. Phys. Oceanogr.,* **27,** 858–870, doi:10.1175/1520-0485(1997)027,0858:DCITMW.2.0.CO;2.

You, Y., 2003: Implications of cabbeling on the formation and transformation mechanism of North Pacific Intermediate Water. *J. Geophys. Res.,* **108,** 3134, doi:10.1029/2001JC001285.

——, N. Suginohara, M. Fukasawa, I. Yasuda, I. Kaneko, H. Yoritaka, and M. Kawamiya, 2000: Roles of the Okhotsk Sea and Gulf of Alaska in forming the North Pacific Intermediate Water. *J. Geophys. Res.,* **105,** 3253–3280, doi:10.1029/1999JC900304.

Yun, J.-Y., and L. D. Talley, 2003: Cabbeling and the density of the North Pacific Intermediate Water quantified by an inverse method. *J. Geophys. Res.,* **108,** 3118, doi:10.1029/2002JC001482.